interleukin (IL)-28B / interferon-lambda 3 (IFN-λ3) gene, which are strongly associated with the efficacy of pegylated interferon-α (PEG-IFN-α) and ribavirin therapy or spontaneous HCV clearance.[1-4]

IFN-λs, or type III IFNs, comprise a family of highly homologous molecules consisting of IFN-λ1 (IL-29), IFN-λ2 (IL-28A), and IFN-λ3 (IL-28B). In clear contrast to type I IFNs, they are released from relatively restricted types of cells, such as hepatocytes, intestinal epithelial cells, or dendritic cells (DCs). Also, the cells that express heterodimeric IFN-λ receptors (IFN-λR1 and IL-10R2) are restricted to cells of epithelial origin, hepatocytes, or DCs.[5] Such limited profiles of cells expressing IFN-λs and their receptors define the biological uniqueness of IFN-λs. It has been shown that IFN-λs convey anti-HCV activity by inducing various interferon-stimulated genes (ISGs),[5] the profiles of which were overlapped but others were distinct from those induced by IFN-α/β. Some investigators showed that the expression of IL-28 in PBMC was higher in subjects with IL-28B major than those with minor; however, the levels of IL-28 transcripts in liver tissue were comparable regardless of IL-28B genotype.[2,6]

At the primary exposure to hosts, HCV maintains high replicative levels in the infected liver, resulting in the induction of IFNs and ISGs. In a case of successful HCV eradication, it is postulated that IFN-α/β and IFN-λ cooperatively induce antiviral ISGs in HCV-infected hepatocytes. It is of particular interest that, in primary human hepatocytes or chimpanzee liver, IFN-λs, but not type I IFNs, are primarily induced after HCV inoculation, the degree of which is closely correlated with the levels of ISGs.[7] These results suggest that hepatic IFN-λ could be a principal driver of ISG induction in response to HCV infection. Nevertheless, the possibility remains that DCs, as a prominent IFN producer in the liver, play significant roles in inducing hepatic ISGs and thereby suppressing HCV replication.

DCs, as immune sentinels, sense specific genomic and/or structural components of pathogens with various pattern recognition receptors and eventually release IFNs and inflammatory cytokines.[8] In general, DCs migrate to the organ where inflammation or cellular apoptosis occurs and alter their function in order to alleviate or exacerbate the disease conditions. Therefore, the phenotypes and/or capacity of liver DCs are deemed to be influenced in the inflamed liver. In humans, the existence of phenotypically and functionally distinct DC subsets has been reported: myeloid DC (mDC) and plasmacytoid DC (pDC).[9] Myeloid DCs predominantly produce IL-12 or tumor necrosis factor alpha (TNF-α) following proinflammatory stimuli, while pDCs release considerable amounts of type I IFNs upon virus infection.[9] The other type of mDCs, mDC2 or BDCA3$^+$(CD141) DCs, have been drawing much attention recently, since human BDCA3$^+$ DCs are reported to be a counterpart of murine CD8a$^+$ DCs.[10] Of particular interest is the report that BDCA3$^+$ DCs have a potent capacity of releasing IFN-λ in response to Toll-like receptor 3 (TLR3) agonist.[11] However, it is still largely unknown whether human BDCA3$^+$ DCs are able to respond to HCV.

Taking these reports into consideration, we hypothesized that human BDCA3$^+$ DCs, as a producer of IFN-λs, have crucial roles in anti-HCV innate immunity. We thus tried to clarify the potential of BDCA3$^+$ DCs in producing type III IFNs by using cell-cultured HCV (HCVcc) or hepatoma cells harboring HCV as stimuli. Our findings show that BDCA3$^+$ DCs are quite a unique DC subset, characterized by a potent and specialized ability to secrete IFN-λs in response to HCV. The ability of BDCA3$^+$ DCs to release IL-28B upon HCV is superior in subjects with IL-28B major (rs8099917, TT) to those with minor (TG or GG) genotype, suggesting that BDCA3$^+$ DCs are one of the key players in IFN-λ-mediated innate immunity.

Patients and Methods

Subjects. This study enrolled 70 healthy volunteers (male/female: 61/9) (age: mean ± standard deviation [SD], 37.3 ± 7.8 years) and 20 patients who underwent surgical resection of liver tumors at Osaka University Hospital (Supporting Table 1). The study was approved by the Ethical Committee of Osaka University Graduate School of Medicine. Written informed consent was obtained from all of them. All healthy volunteers were negative for HCV, hepatitis B virus (HBV), and human immunodeficiency virus (HIV) and had no apparent history of liver, autoimmune, or malignant diseases.

Address reprint requests to: Tatsuya Kanto, M.D., Ph.D., Department of Gastroenterology and Hepatology, Osaka University Graduate School of Medicine, 2-2 Yamadaoka, Suita, 565-0871 Japan. E-mail: kantot@gh.med.osaka-u.ac.jp; fax: +81-6-6879-3629.

View this article online at wileyonlinelibrary.com.
DOI 10.1002/hep.26182
Potential conflict of interest: Nothing to report.
Additional Supporting Information may be found in the online version of this article.

Reagents. The specifications of all antibodies used for FACS or cell sorting TLR-specific synthetic agonists, pharmacological reagents, and inhibitory peptides are listed in the Supporting Materials.

Separation of DCs from PBMC or Intrahepatic Lymphocytes. We collected 400 mL of blood from each healthy volunteer and processed them for PBMCs. Noncancerous liver tissues were obtained from patients who underwent resection of liver tumors (Supporting Table 1). For the collection of intrahepatic lymphocytes (IHLs), liver tissues were washed thoroughly with phosphate-buffered saline to remove the peripheral blood adhering to the tissue and ground gently. After Lin-negative ($CD3^-$, $CD14^-$, $CD19^-$, and $CD56^-$) cells were obtained by the MACS system, each DC subset with the defined phenotype was sorted separately under FACS Aria (BD). The purity was more than 98%, as assessed by FACS Canto II (BD). Sorted DCs were cultured at 2.5×10^4/well on 96-well culture plates.

Immunofluorescence Staining of Human Liver Tissue. Tissue specimens were obtained from surgical resections of noncancerous liver from the patients as described above. Briefly, the 5-mm sections were incubated with the following antibodies: mouse biotinylated antihuman BDCA3 antibody (Miltenyi-Biotec), and mouse antihuman CLEC9A antibody (Biolegend) and subsequently with secondary goat antirabbit Alexa Fluor488 or goat antimouse Alexa Fluor594 (Invitrogen, Molecular Probes) antibodies. Cell nuclei were counterstained with Dapi-Fluoromount-GTM (Southern Biotech, Birmingham, AL). The stained tissues were analyzed by fluorescence microscopy (Model BZ-9000; Keyence, Osaka, Japan).

Cells and Viruses. The *in vitro* transcribed RNA of the JFH-1 strain of HCV was introduced into FT3-7 cells[12] or Huh7.5.1 cells. The stocks of HCVcc were generated by concentration of the medium from JFH-1-infected FT3-7 cells. The virus titers were determined by focus forming assay.[13] The control medium was generated by concentration of the medium from HCV-uninfected FT3-7 cells. Infectious JEVs were generated from the expression plasmid (pMWJEATG1) as reported.[14] HSV (KOS) was a generous gift from Dr. K. Ueda (Osaka University). Huh7.5.1 cells transduced with HCV JFH-1 strain was used for the coculture with DCs. The transcripts of ISGs in Huh7.5.1 were examined by reverse-transcription polymerase chain reaction (RT-PCR) methods using gene-specific primers and probes (Applied Biosystems, Foster City, CA).

Secretion Assays. IL-28B/IFN-λ3 was quantified by a newly developed chemiluminescence enzyme immunoassay (CLEIA) system.[15] IL-29/IFN-λ1, IL-28A/IFN-λ2, and IFN-β were assayed by commercially available enzyme-linked immunosorbent assay (ELISA) kits (eBioscience, R&D, and PBL, respectively). IFN-α was measured by cytometric beads array kits (BD) according to the manufacturer's instructions.

Statistical Analysis. The differences between two groups were assessed by the Mann-Whitney nonparametric U test. Multiple comparisons between more than two groups were analyzed by the Kruskal-Wallis nonparametric test. Paired t tests were used to compare differences in paired samples. All the analyses were performed using GraphPad Prism software (San Diego, CA).

Results

Human BDCA3$^+$ DCs Are Phenotypically Distinct from pDCs and mDCs. We defined $BDCA3^+$ DCs as $Lin^-HLA\text{-}DR^+BDCA3^{high+}$ cells (Fig. 1A, left, middle), and pDCs and mDCs by the patterns of CD11c and CD123 expressions (Fig. 1A, right). The level of CD86 on pDCs or mDCs is comparatively higher than those on $BDCA3^+$ DCs (Fig. 1B). The expression of CD81 is higher on $BDCA3^+$ DCs than on pDCs and mDCs (Fig. 1B, Supporting Fig. S1). CLEC9A, a member of C-type lectin, is expressed specifically on $BDCA3^+$ DCs as reported elsewhere,[16] but not on pDCs and mDCs (Fig. 1B).

Liver BDCA3$^+$ DCs Are More Mature than the Counterparts in the Periphery. $BDCA3^+$ DCs in infiltrated hepatic lymphocytes (IHLs) are all positive for CLEC9A, but liver pDCs or mDCs are not (data not shown). The levels of CD40, CD80, CD83, and CD86 on liver $BDCA3^+$ DCs are higher than those on the peripheral counterparts, suggesting that $BDCA3^+$ DCs are more mature in the liver compared to those in the periphery (Fig. 1C).

In order to confirm that $BDCA3^+$ DCs are localized in the liver, we stained the cells with immunofluorescence antibodies (Abs) in noncancerous liver tissues. Liver $BDCA3^+$ DCs were defined as $BDCA3^+$ $CLEC9A^+$ cells (Fig. 1D). Most of the cells were found near the vascular compartment or in sinusoid or the space of Disse of the liver tissue.

BDCA3$^+$ DCs Are Scarce in PBMCs but More Abundant in the Liver. The percentages of $BDCA3^+$ DCs in PBMCs were much lower than those of the other DC subsets ($BDCA3^+$ DCs, pDCs and mDCs, mean $\pm$ SD [%], 0.054 ± 0.044, 0.27 ± 0.21 and 1.30 ± 0.65) (Fig. 2A). The percentages of $BDCA3^+$ DCs in IHLs were lower than those of the others ($BDCA3^+$ DCs, pDCs, and mDCs, mean $\pm$ SD [%],

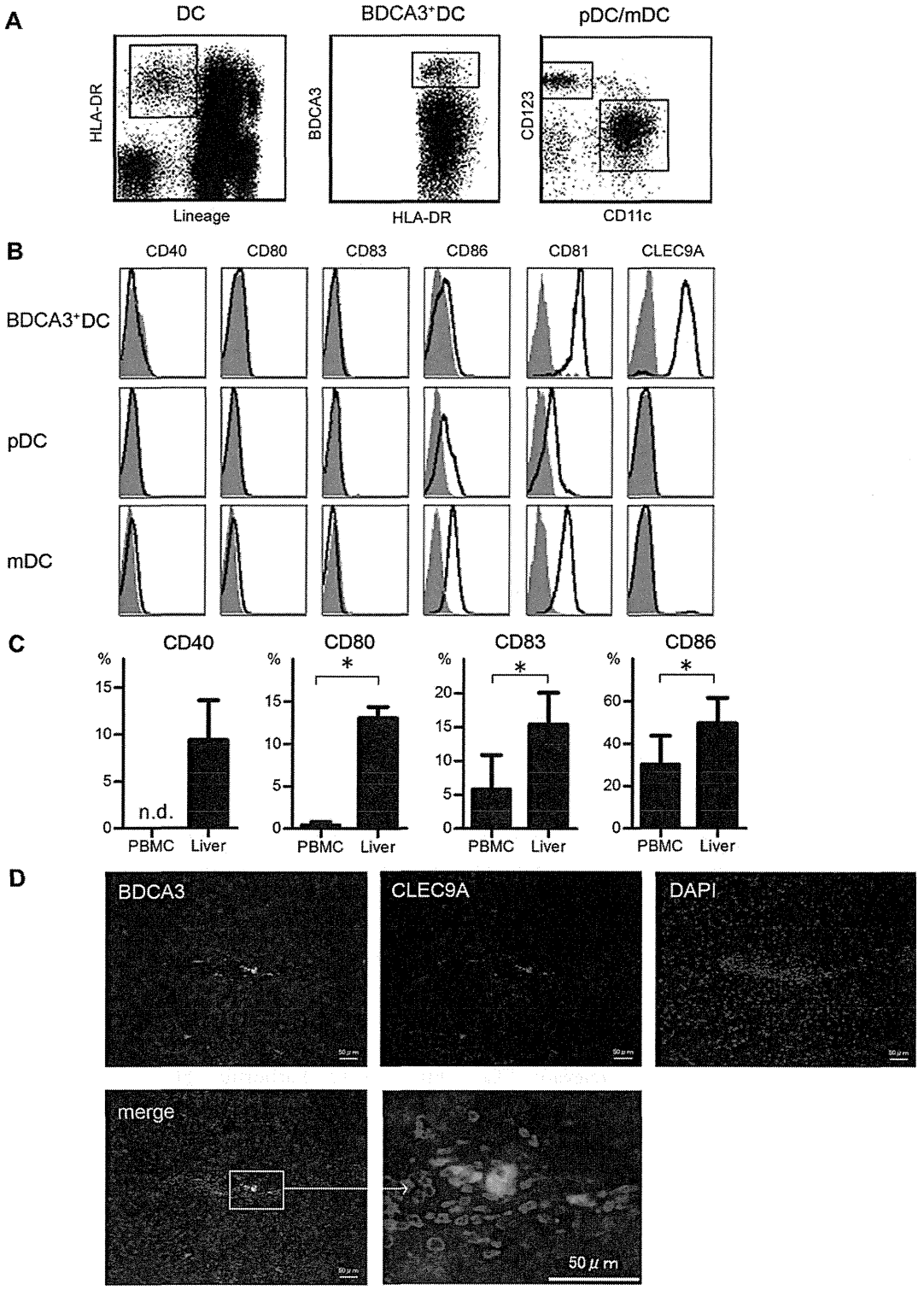

Fig. 1. Identification and phenotypic analyses of peripheral blood and intrahepatic BDCA3$^+$ DCs. (A) We defined BDCA3$^+$ DCs as Lineage$^-$HLA-DR$^+$BDCA3^{high+} cells (middle), pDCs as Lineage$^-$HLA-DR$^+$CD11c$^-$CD123^{high+} cells, and mDCs as Lineage$^-$HLA-DR$^+$CD11c$^+$CD123^{low+} cells (right). (B) The expressions of CD40, CD80, CD83, CD86, CD81, and CLEC9A on each DC subset in peripheral blood are shown. Representative results of five donors are shown in the histograms. Filled gray histograms depict data with isotype Abs, and open black ones are those with specific Abs. (C) The expressions of costimulatory molecules on BDCA3$^+$ DCs were compared between in PBMCs and in the liver. The results are shown as the percentage of positive cells. Results are the mean ± SEM from four independent experiments. *$P < 0.05$ by paired t test. (D) The staining for BDCA3 (green), CLEC9A (red) identifies BDCA3$^+$ DCs (merge, BDCA3$^+$CLEC9A$^+$) in human liver tissues. Representative results of the noncancerous liver samples are shown. BDCA, blood dendritic cell antigen; pDC, plasmacytoid DC; mDC, myeloid DC; CLEC9A, C-type lectin 9A.

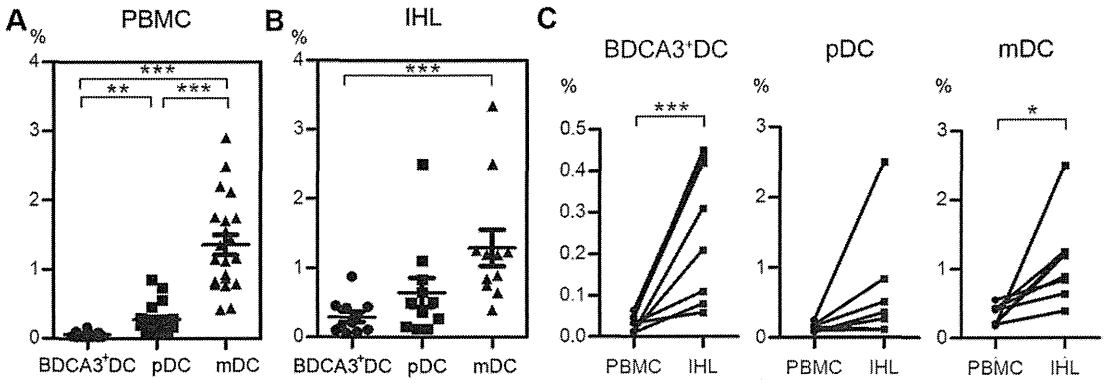

Fig. 2. Analysis of frequency of DC subsets in the peripheral blood and in the liver. Frequencies of BDCA3$^+$ DCs, pDCs, and mDCs in PBMCs (21 healthy subjects) (A) or in the intrahepatic lymphocytes (IHLs) (11 patients who had undergone surgical resection of tumors) (B) are shown. Horizontal bars depict the mean ± SD. $^{**}P < 0.005$; $^{***}P < 0.0005$ by Kruskal-Wallis test. (C) The paired comparisons of the frequencies of DC subsets between in PBMCs and in IHLs. the results of eight patients whose PBMCs and IHLs were obtained simultaneously are shown. $^{*}P < 0.05$; $^{***}P < 0.0005$ by paired *t* test. IHLs, intrahepatic lymphocytes; pDC and mDC, see Fig. 1.

0.29 ± 0.25, 0.65 ± 0.69 and 1.2 ± 0.94) (Fig. 2B). The percentages of BDCA3$^+$ DCs in the IHLs were significantly higher than those in PBMCs from relevant donors (Fig. 2C). Such relative abundance of BDCA3$^+$ DCs in the liver over that in the periphery was observed regardless of the etiology of the liver disease (Supporting Table 1).

BDCA3$^+$ DCs Produce a Large Amount of IFN-λs upon Poly IC Stimulation. We compared DC subsets for their abilities to produce IL-29/IFN-λ1, IL-28A/IFN-λ2, IL-28B/IFN-λ3, IFN-β, and IFN-α in response to TLR agonists. Approximately 4.0×10^4 of BDCA3$^+$ DCs were recoverable from 400 mL of donated blood from healthy volunteers. We fixed the number of DCs at 2.5×10^4 cells/100 mL for comparison in the following experiments.

BDCA3$^+$ DCs have been reported to express mRNA for TLR1, 2, 3, 6, 8, and 10.[17] First, we quantified IL-28B/IFN-λ3 as a representative for IFN-λs after stimulation of BDCA3$^+$ DCs with relevant TLR agonists. We confirmed that BDCA3$^+$ DCs released IL-28B robustly in response to TLR3 agonist/poly IC but not to other TLR agonists (Fig. S2). In contrast, pDCs produced IL-28B in response to TLR9 agonist/CpG but much lesser to other agonists (Fig. S2). Next, we compared the capabilities of DCs inducing IFN-λs and IFN-β genes in response to relevant TLR agonists. BDCA3$^+$ DCs expressed extremely high levels of IL-29, IL-28A, and IL-28B transcripts compared to other DCs, whereas pDCs induced a higher level of IFN-β than other DCs (Fig. S3A).

Similar results were obtained with the protein levels of IFN-λs, IFN-β, and IFN-α released from DC subsets stimulated with TLR agonists. BDCA3$^+$ DCs produce significantly higher levels of IL-29, IL-28B, and IL-28A than the other DC subsets. In clear contrast, pDCs release a significantly larger amount of IFN-β and IFN-α than BDCA3$^+$ DCs or mDCs (Fig. 3A, Fig. S3B). As for the relationship among the quantity of IFN-λ subtypes from poly IC-stimulated BDCA3$^+$ DCs, the levels of IL-29/IFN-λ1 and IL-28B/IFN-λ3 were positively correlated ($R^2 = 0.76$, $P < 0.05$), and those of IL-28A/IFN-λ2 and IL-28B/IFN-λ3 were positively correlated as well ($R^2 = 0.84$, $P < 0.0005$), respectively (Fig. S3C). These results show that the transcription and translation machineries of IFN-λs may be overlapped among IFN-λ subtypes in BDCA3$^+$ DCs upon poly IC stimulation.

Liver BDCA3$^+$ DCs sorted from IHLs possess the ability to produce IL-28B in response to poly IC (Fig. 3B), showing that they are comparably functional. In response to poly IC, BDCA3$^+$ DCs were capable of producing inflammatory cytokines as well, such as TNF-α, IL-6, and IL-12p70 (Fig. S4A). By using Huh7 cells harboring HCV subgenomic replicons (HCV-N, genotype 1b), we confirmed that the supernatants from poly IC-stimulated BDCA3$^+$ DCs suppressed HCV replication in an IL-28B concentration-dependent manner (Fig. S4B). Therefore, poly IC-stimulated BDCA3$^+$ DCs are capable of producing biologically active substances suppressing HCV replication, some part of which may be mediated by IFN-λs.

BDCA3$^+$ DCs Produce IL-28B upon HCVcc or HCV/JFH-1-Transfected Huh7.5.1 Cells. We stimulated freshly isolated BDCA3$^+$ DCs, pDCs and mDCs with infectious viruses, such as HCVcc, Japanese encephalitis virus (JEV), and herpes simplex virus (HSV). In preliminary experiments, we confirmed that HCVcc stimulated BDCA3$^+$ DCs to release IL-28B in a dose-dependent manner (Fig. S5). BDCA3$^+$ DCs

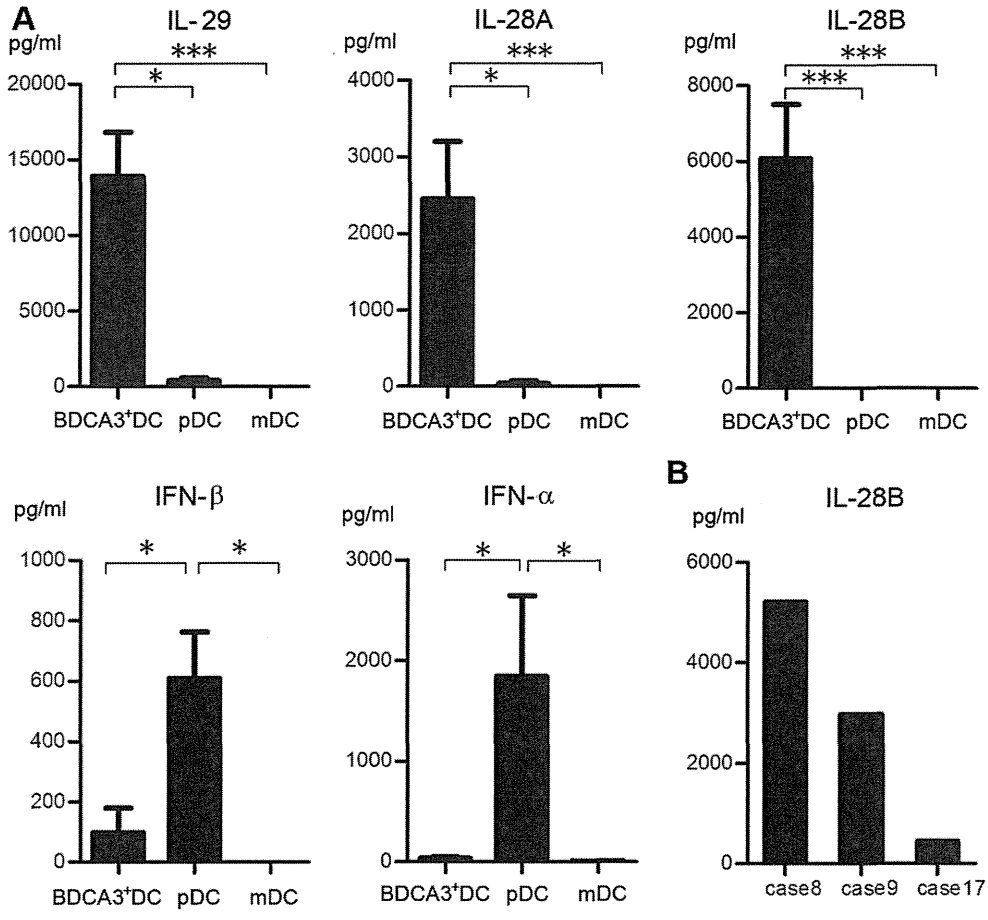

Fig. 3. BDCA3$^+$ DCs recovered from peripheral blood or intrahepatic lymphocytes produce large amounts of IL-29/IFN-λ1, IL-28A/IFN-λ2, and IL-28B/IFN-λ3 in response to poly IC. (A) BDCA3$^+$ DCs and mDCs were cultured at 2.5×10^4 cells with 25 mg/mL poly IC, and pDCs were with 5 mM CPG for 24 hours. The supernatants were examined for IL-29, IL-28A, IL-28B, IFN-β and IFN-α. Results are shown as mean $\pm$ SEM from 15 experiments. *$P < 0.05$; ***$P < 0.0005$ by Kruskal-Wallis test. (B) For the IL-28B production, BDCA3$^+$ DCs in intrahepatic lymphocytes were cultured at 2.5×10^4 cells with 25 mg/mL poly IC for 24 hours. The samples of cases 8 and 9 were obtained from patients with non-B, non-C liver disease and that of case 17 was from an HCV-infected patient (Supporting Table 1).

produced a large amount of IL-28B upon exposure to HCVcc and released a lower amount of IFN-α upon HCVcc or HSV (Fig. 4A). In contrast, pDCs produced a large amount of IFN-α in response to HCVcc and HSV and a much lower level of IL-28B upon HCVcc (Fig. S6). In mDCs, IL-28B and IFN-α were not detectable with any of these viruses (data not shown).

BDCA3$^+$ DCs produced significantly higher levels of IL-28B than the other DCs upon HCVcc stimulation (Fig. 4B). By contrast, HCVcc-stimulated pDCs released significantly larger amounts of IFN-β and IFN-α than the other subsets (Fig. 4B). Liver BDCA3$^+$ DCs were capable of producing IL-28B in response to HCVcc (Fig. 4C). These results show that, upon HCVcc stimulation, BDCA3$^+$ DCs produce more IFN-λs and pDCs release more IFN-β and IFN-α than the other DC subsets, respectively. Taking a clinical impact of IL-28B genotypes on HCV eradication into consideration, we focused on IL-28B/IFN-λ3 as a representative for IFN-λs in the following experiments.

In a coculture with JFH-1-infected Huh7.5.1 cells, BDCA3$^+$ DCs profoundly released IL-29, IL-28A, and IL-28B (Fig. 4D, the results of IL-29 and IL-28A, not shown), whereas BDCA3$^+$ DCs failed to respond to Huh7.5.1 cells lacking HCV/JFH-1, showing that IL-28B production from BDCA3$^+$ DCs is dependent on HCV genome (Fig. 4D). In the absence of BDCA3$^+$ DCs, IL-28B is undetectable in the supernatant from JFH-1-infected Huh7.5.1 cells, demonstrating that BDCA3$^+$ DCs, not HCV-replicating Huh7.5.1 cells, produce detectable amount of IL-28B (Fig. 4D). In the coculture, BDCA3$^+$ DCs comparably released IL-28B either in the presence or the absence of transwells, suggesting that cell-to-cell contact between DCs and Huh7.5.1 cells is dispensable for IL-28B response (Fig. 4E). In parallel with the quantity of IL-28B in the coculture, ISG15 was significantly induced only in JFH-1-infected Huh7.5.1 cells cocultured with BDCA3$^+$ DCs (Fig. 4F). A strong induction was observed with other ISGs in JFH-1-infected Huh7.5.1 in the presence of BDCA3$^+$ DCs, such as IFIT1, MxA, RSD2, IP-10, and USP18 (Fig. S7). The results clearly show that BDCA3$^+$ DCs are capable of producing large amounts of IFN-λs in response to cellular or cell-free HCV, thereby inducing various ISGs in bystander liver cells.

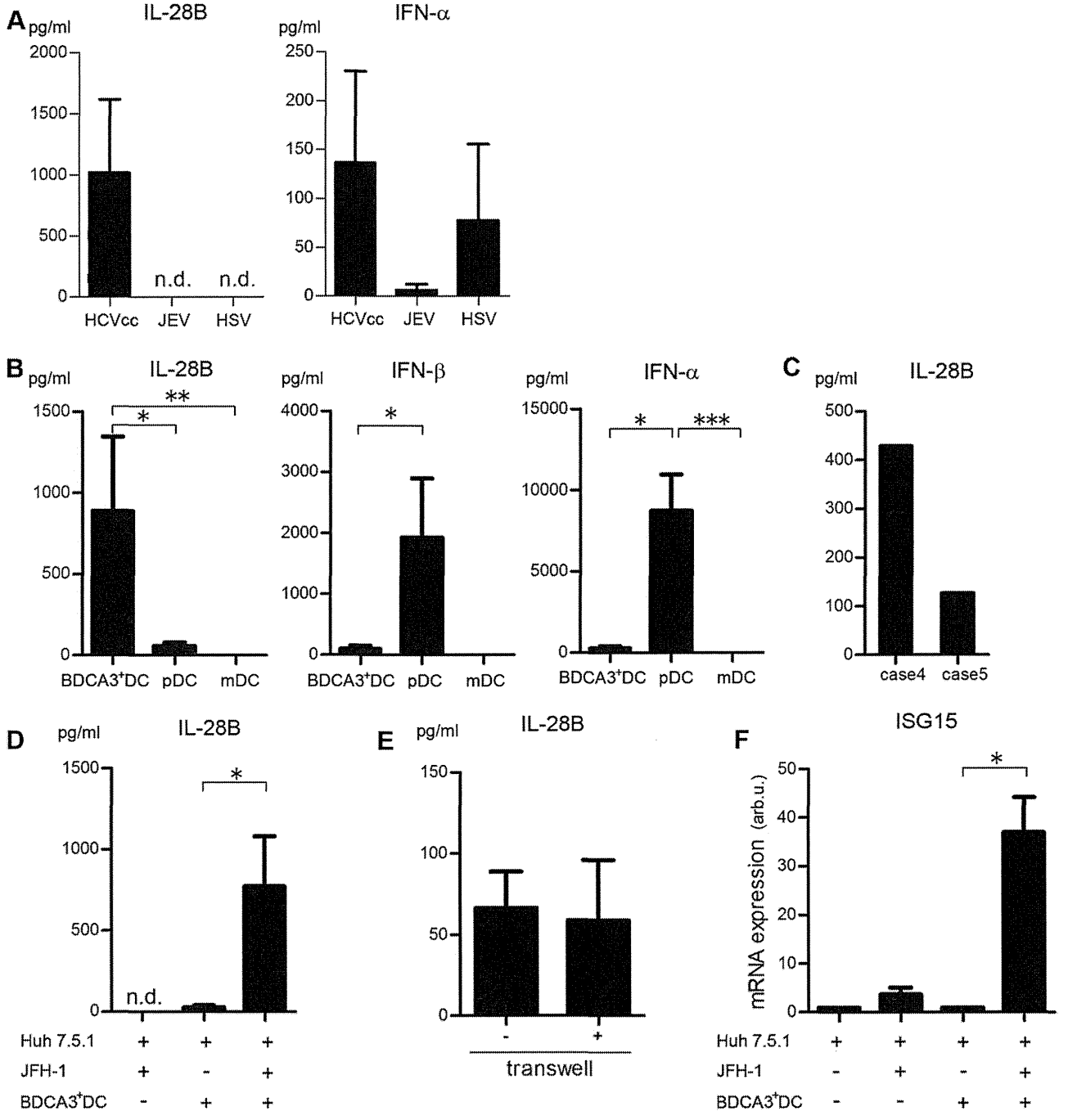

Fig. 4. BDCA3$^+$ DCs produce IL-29, IL-28A, and IL-28B upon cell-cultured HCV or HCV/JFH-1-transfected Huh7.5.1 cells, thereby inducing ISG. (A) BDCA3$^+$ DCs were cultured at 2.5 $\times$ 10^4 cells for 24 hours with HCVcc, JEV, or HSV at a multiplicity of infection (MOI) of 10. Results are shown as mean $\pm$ SEM from six experiments. n.d.; not detected. (B) BDCA3$^+$ DCs, pDCs, and mDCs were cultured at 2.5 $\times$ 10^4 cells for 24 hours with HCVcc at an MOI of 10. The results are shown as mean $\pm$ SEM from 11 experiments. *$P < 0.05$; **$P < 0.0005$; ***$P < 0.0005$ by Kruskal-Wallis test. (C) BDCA3$^+$ DCs recovered from intrahepatic lymphocytes were cultured at 2.5 $\times$ 10^4 cells for 24 hours with HCVcc at an MOI of 10. Both of the samples (cases 4 and 5) were obtained from patients with non-B, non-C liver disease. (D,E) BDCA3$^+$ DCs were cocultured at 2.5 $\times$ 10^4 cells with JFH-1-transfected (MOI = 2) or -untransfected Huh7.5.1 cells for 24 hours. The supernatants of JFH-1-transfected Huh7.5.1.cells without BDCA3$^+$ DCs were also examined. In some experiments of the coculture with JFH-1-transfected Huh7.5.1 cells and BDCA3$^+$ DCs, transwells were inserted into the wells (E). Results are shown as mean $\pm$ SEM from five experiments. *$P < 0.05$ by paired t test. (F) BDCA3$^+$ DCs were cocultured at 2.5 $\times$ 10^4 cells with JFH-1-transfected Huh7.5.1 cells (MOI = 2) or -untransfected Huh7.5.1 cells for 24 hours. The Huh7.5.1.cells were harvested and subjected to real-time RT-PCR analyses for ISG15 expression. The results are shown as mean $\pm$ SEM from five experiments. *$P < 0.05$ by paired t test. HCVcc, cell-cultured HCV; JEV, Japanese encephalitis virus; HSV, herpes simplex virus.

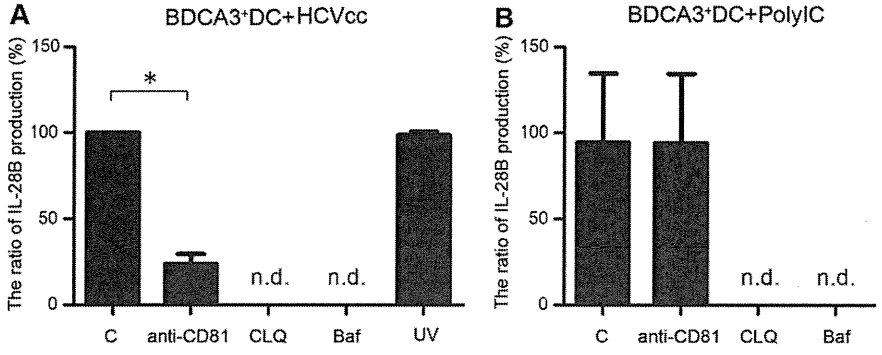

Fig. 5. The CD81 and endosome acidification is involved in the production of IL-28B from HCV-stimulated BDCA3$^+$ DCs, but HCV replication is not necessary. (A,B) BDCA3$^+$ DCs were cultured at 2.5 $\times$ 10^4 cells with HCVcc at an MOI of 10 (A) or poly IC (25 μg/mL) (B). In some experiments, UV-irradiated HCVcc was used at the same MOI, and BDCA3$^+$ DCs were treated with anti-CD81Ab (5 mg/mL), chloroquine (10 mM), or bafilomycin A1 (25 nM). The results are expressed as ratios of IL-28B quantity with or without the treatments. They are shown as mean $\pm$ SEM from five experiments. *$P < 0.05$ by paired t test. C, control; CLQ, treatment with chloroquine; Baf, treatment with bafilomycin A1; UV, ultraviolet-irradiated HCVcc; n.d., not detected.

CD81 and Endosome Acidification Are Involved in IL-28B Production from HCV-Stimulated BDCA3$^+$ DCs, but HCV Replication Is Not Involved. It is not known whether HCV entry and subsequent replication in DCs is involved or not in IFN response.[18,19] To test this, BDCA3$^+$ DCs were inoculated with UV-irradiated, replication-defective HCVcc. We confirmed that UV exposure under the current conditions is sufficient to negate HCVcc replication in Huh7.5.1 cells, as demonstrated by the lack of expression of NS5A after inoculation (data not shown). BDCA3$^+$ DCs produced comparable levels of IL-28B with UV-treated HCVcc, indicating that active HCV replication is not necessary for IL-28B production (Fig. 5A).

We next examined whether or not the association of HCVcc with BDCA3$^+$ DCs by CD81 is required for IL-28B production. It has been reported that the E2 region of HCV structural protein is associated with CD81 on cells when HCV enters susceptible cells.[13,20] We confirmed that all DC subsets express CD81, the degree of which was most significant on BDCA3$^+$ DCs (Fig. 1B, Fig. S1). Masking of CD81 with Ab significantly impaired IL-28B production from HCVcc-stimulated BDCA3$^+$ DCs in a dose-dependent manner (Fig. 5A, Fig. S8), suggesting that HCV-E2 and CD81 interaction is involved in the induction. The treatment of poly IC-stimulated BDCA3$^+$ DCs with anti-CD81 Ab failed to suppress IL-28B production (Fig. 5B).

HCV enters the target cells, which is followed by fusion steps within acidic endosome compartments. Chloroquine and bafilomycin A1 are well-known and broadly used inhibitors of endosome TLRs, which are reported to be capable of blocking TLR3 response in human monocyte-derived DC.[21,22] In our study, the treatment of BDCA3$^+$ DCs with chloroquine, bafilomycin A1, or NH4Cl significantly suppressed their IL-28B production either in response to HCVcc or poly IC (Fig. 5A,B, NH4Cl, data not shown). These results suggest that the endosome acidification is involved in HCVcc- or poly IC-stimulated BDCA3$^+$ DCs to produce IL-28B. The similar results were obtained with HCVcc-stimulated pDCs for the production of IL-28B (Fig. S9). We validated that such concentration of chloroquine (10 mM) and bafilomycin A1 (25 nM) did not reduce the viability of BDCA3$^+$ DCs (Fig. S10).

BDCA3$^+$ DCs Produce IL-28B in Response to HCVcc by a TIR-Domain-Containing Adapter-Inducing Interferon-β (TRIF)-Dependent Mechanism. TRIF/TICAM-1, a TIR domain-containing adaptor, is known to be essential for the TLR3-mediated pathway.[23] In order to elucidate whether TLR3-dependent pathway is involved or not in IL-28B response of BDCA3$^+$ DCs, we added the cell-permeable TRIF-specific inhibitory peptide (Invivogen) or the control peptide to poly IC- or HCVcc-stimulated BDCA3$^+$ DCs. Of particular interest, the TRIF-specific inhibitor peptide, but not the control one, significantly suppressed IL-28B production from poly IC- or HCVcc-stimulated BDCA3$^+$ DCs (Fig. 6A,B). In clear contrast, the TRIF-specific inhibitor failed to suppress IL-28B from HCVcc-stimulated pDCs (Fig. 6C), suggesting that pDCs recognize HCVcc in an endosome-dependent but TRIF-independent pathway. These results show that BDCA3$^+$ DCs may recognize HCVcc by way of the TRIF-dependent pathway to produce IL-28B.

BDCA3$^+$ DCs in Subjects with IL-28B Major Genotype Produce More IL-28B in Response to HCV than Those with IL-28B Minor Type. In order to compare the ability of BDCA3$^+$ DCs to release IL-28B in healthy subjects between IL28B major (rs8099917, TT)

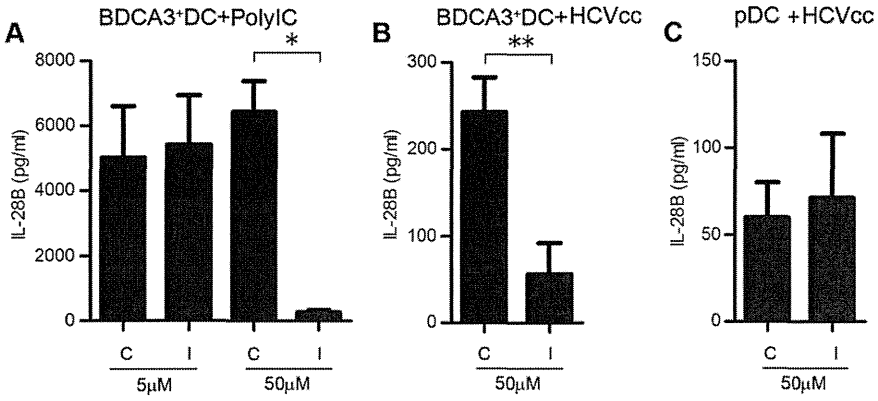

Fig. 6. BDCA3$^+$ DCs produce IL-28B upon HCVcc stimulation in a TRIF-dependent mechanism. BDCA3$^+$ DCs or pDCs had been treated with 5 or 50 mM TRIF inhibitory peptide or control peptide for 2 hours. Subsequently, BDCA3$^+$ DCs were stimulated with Poly IC (25 μg/mL) or HCVcc (MOI = 10), and pDCs were stimulated with HCVcc (MOI = 10), respectively. IL-28B was quantified by ELISA. They are shown as mean ± SEM from five experiments. *$P < 0.05$ by paired t test. C, TRIF control peptide; I, TRIF inhibitory peptide.

and minor hetero (TG) genotypes, we stimulated BDCA3$^+$ DCs of the identical subjects with poly IC (25 mg/mL, 2.5 mg/mL, 0.25 mg/mL), HCVcc or JFH-1-infected Huh 7.5.1, and subjected them to ELISA. The levels of IL-28B production by poly IC-stimulated BDCA3$^+$ DCs were comparable between subjects with IL-28B major and minor type (Fig. 7A). Similar results were obtained with the lesser concentrations of poly IC (Fig. S11). Of particular interest, in response to HCVcc or JFH-1 Huh7.5.1 cells, the levels of IL-28B from BDCA3$^+$ DCs were significantly higher in subjects with IL-28B major than those with minor type (Fig. 7B,C, S12).

Discussion

In this study we demonstrated that human BDCA3$^+$ DCs (1) are present at an extremely low frequency in PBMC but are accumulated in the liver; (2) are capable of producing IL-29/IFN-λ1, IL-28A/IFN-λ2, and IL-28B/IFN-λ3 robustly in response to HCV; (3) recognize HCV by a CD81-, endosome acidification and TRIF-dependent mechanism; and (4) produce larger amounts of IFN-λs upon HCV stimulation in subjects with IL-28B major genotype (rs8099917, TT). These characteristics of BDCA3$^+$ DCs are quite unique in comparison with other DC repertoires in the settings of HCV infection.

At the steady state, the frequency of DCs in the periphery is relatively lower than that of the other immune cells. However, under disease conditions or physiological stress, activated DCs dynamically migrate to the site where they are required to be functional. However, it remains obscure whether functional BDCA3$^+$ DCs exist or not in the liver. We identified BDCA3$^+$CLEC9A$^+$ cells in the liver tissue (Fig. 1D). In a paired frequency analysis of BDCA3$^+$ DCs between in PBMCs and in IHLs, the cells are more abundant in the liver. The phenotypes of liver BDCA3$^+$ DCs were more mature than the PBMC counterparts. In support of our observations, a recent publication showed that CD141$^+$ (BDCA3$^+$) DCs are accumulated and more mature in the liver, the trend of which is more in HCV-infected liver.[24] We confirmed that liver BDCA3$^+$ DCs are functional, capable of releasing IFN-λs in response to poly IC or HCVcc.

BDCA3$^+$ DCs were able to produce large amounts of IFN-λs but much less IFN-β or IFN-α upon TLR3 stimulation. In contrast, in response to TLR9 agonist,

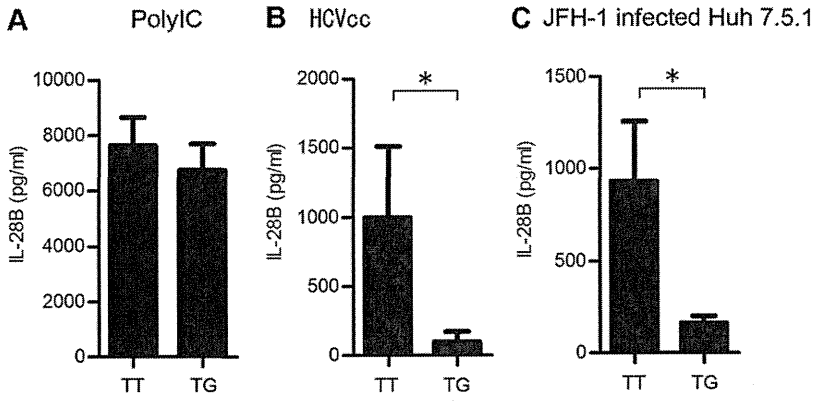

Fig. 7. In response to HCVcc, BDCA3$^+$ DCs of healthy donors with IL-28B major genotype (rs8099917, TT) produced more IL-28B than those with minor type (TG). BDCA3$^+$ DCs of healthy donors with IL-28B TT (rs8099917) or TG genotype were cultured at 2.5 × 10^4 cells with 25 mg/mL poly IC (A), with HCVcc at an MOI of 10 (B), or with JFH-1-infected Huh 7.5.1 cells (C) for 24 hours. The supernatants were subjected to IL-28B ELISA. The same healthy donors were examined for distinct stimuli. The results are the mean ± SEM from 15 donors with TT and 8 with TG, respectively. *$P < 0.05$ by Mann-Whitney U test.

pDCs released large amounts of IFN-β and IFN-α but much less IFN-λs. Such distinctive patterns of IFN response between BDCA3$^+$ DCs and pDCs are of particular interest. It has been reported that interferon regulatory factor (IRF)-3, IRF-7, or nuclear factor kappa B (NF-κB) are involved in IFN-β and IFN-λ1, while IRF-7 and NF-κB are involved in IFN-α and IFN-λ2/λ3.[5] Presumably, the stimuli with TLR3/retinoic acid-inducible gene-I (RIG-I) (poly IC) or TLR9 agonist (CpG-DNA) in DCs are destined to activate these transcription factors, resulting in the induction of both types of IFN at comparable levels. However, the results of the present study did not agree with such overlapping transcription factors for IFN-λs, IFN-β, and IFN-α. Two possible explanations exist for different levels of IFN-λs and IFN-α production by BDCA3$^+$ DCs and pDCs. First, the transcription factors required for full activation of IFN genes may differ according to the difference of DC subsets. The second possibility is that since type III IFN genes have multiple exons, they are potentially regulated by posttranscriptional mechanisms. Thus, it is possible that such genetic and/or posttranscriptional regulation is distinctively executed between BDCA3$^+$ DCs and pDCs. Comprehensive analysis of gene profiles downstream of TLRs or RIG-I in BDCA3$^+$ DCs should offer some information on this important issue.

BDCA3$^+$ DCs were found to be more sensitive to HCVcc than JEV or HSV in IL-28B/IFN-λ3 production. Such different strengths of IL-28B in BDCA3$^+$ DCs depending on the virus suggest that different receptors are involved in virus recognition. Again, the question arises of why BDCA3$^+$ DCs produce large amounts of IFN-λs compared to the amounts produced by pDCs in response to HCVcc. Considering that IRF-7 and NF-κB are involved in the transcription of the IL-28B gene, it is possible that BDCA3$^+$ DCs successfully activate both transcription factors upon HCVcc for maximizing IL-28B, whereas pDCs fail to do so. In support for this possibility, in pDCs it is reported that NF-κB is not properly activated upon HCVcc or hepatoma cell-derived HCV stimulations.[25]

In the present study we demonstrated that HCV entry into BDCA3$^+$ DCs through CD81 and subsequent endosome acidification are critically involved in IL-28B responses. Involvement of TRIF-dependent pathways in IL-28B production was shown by the significant inhibition of IL-28B with TRIF inhibitor. Nevertheless, active HCV replication in the cells is not required. Based on our data, we considered that BDCA3$^+$ DCs recognize HCV genome mainly by an endosome and TRIF-dependent mechanism. Although the results with UV-irradiated HCVcc, anti-CD81 blocking Ab, and chloroquine were quite similar, the TRIF-specific inhibitor failed to suppress IL-28B from pDCs (Fig. 6, Fig. S9).

In the coculture with JFH-transfected Huh7.5.1 cells, BDCA3$^+$ DCs presumably receive some signals for IL-28B production by way of cell-to-cell dependent and independent mechanisms. In the present study, most of the stimuli to BDCA3$^+$ DCs for IL-28B production may be the released HCVcc from Huh7.5.1 cells, judging from the inability of suppression with transwells. However, a contribution of contact-dependent mechanisms cannot be excluded in the coculture experiments. HCV genome is transmissible from infected hepatocytes to uninfected ones through tight junction molecules, such as claudin-1 and occuludin. Further investigation is needed to clarify whether such cell-to-cell transmission of viral genome is operated or not in BDCA3$^+$ DCs.

The relationship between IL-28B expression and the induction of ISGs has been drawing much research attention. In primary human hepatocytes, it is reported that HCV primarily induces IFN-λ, instead of type-I IFNs, subsequently enhancing ISG expression.[7] Of particular interest is that the level of hepatic IFN-λs is closely correlated with the strength of ISG response.[26] These reports strongly suggest that hepatic IFN-λs are a crucial driver of ISG induction and subsequent HCV eradication. Besides, it is likely that BDCA3$^+$ DCs, as a bystander IFN-λ producer in the liver, have a significant impact on hepatic ISG induction. In support of this possibility, we demonstrated in this study that BDCA3$^+$ DCs are capable of producing large amounts of IFN-λs in response to HCV, thereby inducing ISGs in the coexisting liver cells.

Controversial results have been reported regarding the relationship between IL28B genotypes and the levels of IL-28 expression. Nevertheless, in chronic hepatitis C patients with IL-28B major genotype, the IL-28 transcripts in PBMCs are reported to be higher than those with minor genotype.[2] In this study, by focusing on a prominent IFN-λ producer (BDCA3$^+$ DCs) and using the assay specific for IL-28B, we showed that the subjects with IL-28B major genotype could respond to HCV by releasing more IL-28B. Of interest, such a superior capacity of BDCA3$^+$ DCs was observed only in response to HCV but not to poly IC. Since the pathways downstream of TLR3-TRIF leading to IL-28B in BDCA3$^+$ DCs should be the same, either HCV or poly IC stimulation, two plausible explanations exist for such a distinct IL-28B response. First, it is possible that distinct epigenetic regulation may be

involved in IL-28B gene according to the IL-28B genotypes. Recently, in influenza virus infection, it is reported that micro-RNA29 and DNA methyltransferase are involved in the cyclooxygenase-2-mediated enhancement of IL-29/IFN-λ1 production.[27] This report supports the possibility that similar epigenetic machineries could be operated as well in HCV-induced IFN-λs production. Second, it is plausible that the efficiency of the stimulation of TLR3-TRIF may be different between the IL-28B genotypes. Since HCV reaches endosome in BDCA3$^+$ DCs by way of the CD81-mediated entry and subsequent endocytosis pathways, the efficiencies of HCV handling and enzyme reactions in endosome may be influential in the subsequent TLR3-TRIF-dependent responses. Certain unknown factors regulating such process may be linked to the IL-28B genotypes. For a comprehensive understanding of the biological importance of IL-28B in HCV infection, such confounding factors, if they exist, need to be explored.

In conclusion, human BDCA3$^+$ DCs, having a tendency to accumulate in the liver, recognize HCV and produce large amounts of IFN-λs. An enhanced IL-28B/IFN-λ3 response of BDCA3$^+$ DCs to HCV in subjects with IL-28B major genotype suggests that BDCA3$^+$ DCs are one of the key players in anti-HCV innate immunity. An exploration of the molecular mechanisms of potent and specialized capacity of BDCA3$^+$ DCs as IFN-λ producer could provide useful information on the development of a natural adjuvant against HCV infection.

References

1. Suppiah V, Moldovan M, Ahlenstiel G, Berg T, Weltman M, Abate ML, et al. IL28B is associated with response to chronic hepatitis C interferon-alpha and ribavirin therapy. Nat Genet 2009;41:1100-1104.
2. Tanaka Y, Nishida N, Sugiyama M, Kurosaki M, Matsuura K, Sakamoto N, et al. Genome-wide association of IL28B with response to pegylated interferon-alpha and ribavirin therapy for chronic hepatitis C. Nat Genet 2009;41:1105-1109.
3. Ge D, Fellay J, Thompson AJ, Simon JS, Shianna KV, Urban TJ, et al. Genetic variation in IL28B predicts hepatitis C treatment-induced viral clearance. Nature 2009;461:399-401.
4. Thomas DL, Thio CL, Martin MP, Qi Y, Ge D, O'Huigin C, et al. Genetic variation in IL28B and spontaneous clearance of hepatitis C virus. Nature 2009;461:798-801.
5. Kotenko SV. IFN-lambdas. Curr Opin Immunol 2011;23:583-590.
6. Urban TJ, Thompson AJ, Bradrick SS, Fellay J, Schuppan D, Cronin KD, et al. IL28B genotype is associated with differential expression of intrahepatic interferon-stimulated genes in patients with chronic hepatitis C. Hepatology 2010;52:1888-1896.
7. Park H, Serti E, Eke O, Muchmore B, Prokunina-Olsson L, Capone S, et al. IL-29 is the dominant type III interferon produced by hepatocytes during acute hepatitis C virus infection. Hepatology 2012;56:2060-2070.
8. Medzhitov R. Recognition of microorganisms and activation of the immune response. Nature 2007;449:819-826.
9. Liu YJ. Dendritic cell subsets and lineages, and their functions in innate and adaptive immunity. Cell 2001;106:259-262.
10. Poulin LF, Salio M, Griessinger E, Anjos-Afonso F, Craciun L, Chen JL, et al. Characterization of human DNGR-1+ BDCA3+ leukocytes as putative equivalents of mouse CD8alpha+ dendritic cells. J Exp Med 2010;207:1261-1271.
11. Lauterbach H, Bathke B, Gilles S, Traidl-Hoffmann C, Luber CA, Fejer G, et al. Mouse CD8alpha+ DCs and human BDCA3+ DCs are major producers of IFN-lambda in response to poly IC. J Exp Med 2010;207:2703-2717.
12. Wakita T, Pietschmann T, Kato T, Date T, Miyamoto M, Zhao Z, et al. Production of infectious hepatitis C virus in tissue culture from a cloned viral genome. Nat Med 2005;11:791-796.
13. Lindenbach BD, Evans MJ, Syder AJ, Wolk B, Tellinghuisen TL, Liu CC, et al. Complete replication of hepatitis C virus in cell culture. Science 2005;309:623-626.
14. Mori Y, Okabayashi T, Yamashita T, Zhao Z, Wakita T, Yasui K, et al. Nuclear localization of Japanese encephalitis virus core protein enhances viral replication. J Virol 2005;79:3448-3458.
15. Sugiyama M, Kimura T, Naito S, Mukaide M, Shinauchi T, Ueno M, et al. Development of interferon lambda 3 specific quantification assay for its mRNA and serum/plasma specimens. Hepatol Res 2012;42:1089-1099.
16. Schreibelt G, Klinkenberg LJ, Cruz LJ, Tacken PJ, Tel J, Kreutz M, et al. The C type lectin receptor CLEC9A mediates antigen uptake and (cross-)presentation by human blood BDCA3+ myeloid dendritic cells. Blood 2012;119:2284-2292.
17. Jongbloed SL, Kassianos AJ, McDonald KJ, Clark GJ, Ju X, Angel CE, et al. Human CD141+ (BDCA-3)+ dendritic cells (DCs) represent a unique myeloid DC subset that cross-presents necrotic cell antigens. J Exp Med 2010;207:1247-1260.
18. Marukian S, Jones CT, Andrus L, Evans MJ, Ritola KD, Charles ED, et al. Cell culture-produced hepatitis C virus does not infect peripheral blood mononuclear cells. Hepatology 2008;48:1843-1850.
19. Liang H, Russell RS, Yonkers NL, McDonald D, Rodriguez B, Harding CV, et al. Differential effects of hepatitis C virus JFH1 on human myeloid and plasmacytoid dendritic cells. J Virol 2009;83:5693-5707.
20. Zhang J, Randall G, Higginbottom A, Monk P, Rice CM, McKeating JA. CD81 is required for hepatitis C virus glycoprotein-mediated viral infection. J Virol 2004;78:1448-1455.
21. Blanchard E, Belouzard S, Goueslain L, Wakita T, Dubuisson J, Wychowski C, et al. Hepatitis C virus entry depends on clathrin-mediated endocytosis. J Virol 2006;80:6964-6972.
22. de Bouteiller O, Merck E, Hasan UA, Hubac S, Benguigui B, Trinchieri G, et al. Recognition of double-stranded RNA by human toll-like receptor 3 and downstream receptor signaling requires multimerization and an acidic pH. J Biol Chem 2005;280:38133-38145.
23. Takeda K, Akira S. TLR signaling pathways. Semin Immunol 2004;16:3-9.
24. Velazquez VM, Hon H, Ibegbu C, Knechtle SJ, Kirk AD, Grakoui A. Hepatic enrichment and activation of myeloid dendritic cells during chronic hepatitis C virus infection. Hepatology 2012;56:2071-2081.
25. Dental C, Florentin J, Aouar B, Gondois-Rey F, Durantel D, Baumert TF, et al. Hepatitis C virus fails to activate NF-kappaB signaling in plasmacytoid dendritic cells. J Virol 2012;86:1090-1096.
26. Thomas E, Gonzalez VD, Li Q, Modi AA, Chen W, Noureddin M, et al. HCV infection induces a unique hepatic innate immune response associated with robust production of type III interferons. Gastroenterology 2012;142:978-988.
27. Fang J, Hao Q, Liu L, Li Y, Wu J, Huo X, Zhu Y. Epigenetic changes mediated by microRNA miR29 activate cyclooxygenase 2 and lambda-1 interferon production during viral infection. J Virol 2012;86:1010-1020.

Journal of proteome research

Article

pubs.acs.org/jpr

Understanding the Biological Context of NS5A–Host Interactions in HCV Infection: A Network-Based Approach

Lokesh P. Tripathi,*[,¶,†] Hiroto Kambara,[¶,‡] Yi-An Chen,[†] Yorihiro Nishimura,[‡] Kohji Moriishi,[‡] Toru Okamoto,[‡] Eiji Morita,[‡] Takayuki Abe,[‡] Yoshio Mori,[‡] Yoshiharu Matsuura,[‡] and Kenji Mizuguchi*[,†,§]

[†]National Institute of Biomedical Innovation, 7-6-8 Saito Asagi, Ibaraki, Osaka, 567-0085, Japan

[‡]Department of Molecular Virology, Research Institute for Microbial Diseases, Osaka University, 3-1 Yamada-Oka, Suita, Osaka, 565-0871, Japan

[§]Graduate School of Frontier Biosciences, Osaka University, 1-3 Yamada-Oka, Suita, Osaka, 565-0871, Japan

Supporting Information

ABSTRACT: Hepatitis C virus (HCV) is a major cause of chronic liver disease. HCV NS5A protein plays an important role in HCV infection through its interactions with other HCV proteins and host factors. In an attempt to further our understanding of the biological context of protein interactions between NS5A and host factors in HCV pathogenesis, we generated an extensive physical interaction map between NS5A and cellular factors. By combining a yeast two-hybrid assay with comprehensive literature mining, we built the NS5A interactome composed of 132 human proteins that interact with NS5A. These interactions were integrated into a high-confidence human protein interactome (HPI) with the help of the TargetMine data warehouse system to infer an overall protein interaction map linking NS5A with the components of the host cellular networks. The NS5A–host interactions that were integrated with the HPI were shown to participate in compact and well-connected cellular networks. Functional analysis of the NS5A "infection" network using TargetMine highlighted cellular pathways associated with immune system, cellular signaling, cell adhesion, cellular growth and death among others, which were significantly targeted by NS5A–host interactions. In addition, cellular assays with in vitro HCV cell culture systems identified two ER-localized host proteins RTN1 and RTN3 as novel regulators of HCV propagation. Our analysis builds upon the present understanding of the role of NS5A protein in HCV pathogenesis and provides potential targets for more effective anti-HCV therapeutic intervention.

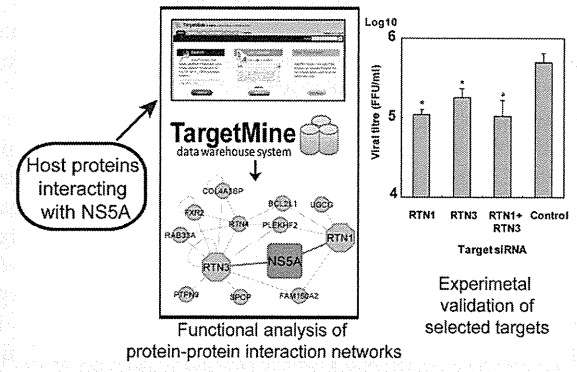

KEYWORDS: *HCV, NS5A, host–pathogen protein–protein interactions, biological network analysis, literature mining, pathway enrichment analysis, siRNA knockdown, target discovery, TargetMine, yeast two-hybrid*

INTRODUCTION

Hepatitis C virus (HCV) causes chronic liver disease including liver steatosis, cirrhosis and hepatocellular carcinoma (HCC) and infects nearly 3% of the world population. HCV possesses a single-stranded RNA genome encoding a 3000 amino acid polyprotein, which is processed by host and viral proteases to yield 10 viral proteins, Core, E1, E2, p7, NS2, NS3, NS4A, NS4B, NS5A and NS5B.[1−5] HCV variants are classified into seven genotypes that display phylogenetic heterogeneity, differences in infectivity and interferon sensitivity.[6,7] However, despite considerable research, a precise understanding of the molecular mechanisms underlying HCV pathology remains elusive.

HCV NS5A protein (hereafter referred to as NS5A) is a RNA binding phosphoprotein, which consists of three domains; domain I includes a zinc-finger motif necessary for HCV replication and an N-terminal membrane anchor region, and the unstructured domains II and III facilitate protein–protein interactions. NS5A plays a critical role in regulating viral replication, production of infectious viral particles, interferon resistance and modulation of apoptosis in HCV pathogenesis via interactions with other HCV proteins and host factors.[8−12] Furthermore, BMS-790052, a small molecule inhibitor of NS5A, is the most potent inhibitor of HCV infection known so far.[13] Consequently, NS5A has emerged as a unique, attractive and promising target for anti-HCV therapy.[14−19] In particular, impairing interactions between NS5A and host factors has been shown to impede HCV infection, which may offer novel anti-HCV therapeutic approaches.[12,20] However, the overall structure and precise functions of NS5A in HCV pathogenesis are poorly understood.

Pathogens such as viruses infect their hosts by interacting with the components of the host cellular networks and

Received: November 30, 2012
Published: May 6, 2013

exploiting the cellular machinery for their survival and propagation. Therefore, elucidating host–pathogen interactions is crucial for a better understanding of pathogenesis.[21−26] Here, we report the host biological processes likely to be influenced by NS5A by virtue of an inferred protein–protein interaction (PPI) network. We describe our integrated approach that combines an experimental yeast two-hybrid (Y2H) assay using NS5A as bait to screen a library of human cDNAs with comprehensive literature mining. The analysis of the NS5A infection network illustrates the functional pathways likely to be influenced by NS5A–host interactions in HCV pathogenesis, thus providing novel insights into the NS5A function in HCV pathogenesis. Furthermore, RTN1 and RTN3, which are endoplasmic reticulum (ER)-localized proteins involved in regulating ER integrity, will be demonstrated as novel regulators of HCV propagation and thus attractive targets for anti-HCV therapy.

■ MATERIALS AND METHODS

Yeast Two-Hybrid Protein Assay

Screening for the genes encoding host proteins that interact with NS5A was performed using the Matchmaker two-hybrid system (Clontech, Palo Alto, CA, USA) as per the manufacturers' specifications. Human adult liver libraries were purchased from Clontech and were cloned into the pAct2 vector (Clontech) and expressed as fusion proteins fused to the Gal4-activation domain (Gal4-AD). Since Y2H requires the bait protein to translocate to the nucleus, the cDNA of the region corresponding to the NS5A encoding amino acids 1973–2419 (excluding the NS5A N-terminal membrane anchor region) within the HCV polyprotein from the J1 strain (genotype 1b)[27] was amplified by polymerase chain reaction (PCR) and was cloned into the pGBKT7 vector (Clontech)[28] and expressed as Gal4-DNA binding domain (Gal4-DB) fusion in the AH109 yeast strain. The human liver libraries were subsequently screened by Y2H using NS5A as bait. A total of 4×10^6 transformants were screened in this manner, and the positive clones (see Supporting Information) were isolated and sequenced to identify the genes coding for the NS5A interacting host factors (Supporting Information, Table S1).

Literature Mining for Pairwise NS5A–Human Interactions

Literature information describing pairwise interactions between NS5A and cellular proteins were extracted from Medline using the PubMed interface and two other information retrieval and extraction tools, EBIMed[29] and Protein Corral. These tools employ an automatic text-mining approach, but we supplemented them with a follow-up manual inspection. All abstracts related to "NS5A" and "HCV NS5A" keywords and interaction verbs (including "interact", "bind", "attach", "associate")[30] were gathered and manually examined to retrieve direct pairwise NS5A–human protein interactions (see Supporting Information, Tables S2, S3, S4, S5a).

Construction of Extended Protein–Protein Interaction Networks

Physical and direct binary interactions between all human proteins were retrieved from BioGRID 3.1.93[31] and iRefindex 9.0[32] databases using TargetMine.[33] TargetMine is an integrated data warehouse that combines different types of biological data and employs an objective protocol to prioritise candidate genes for further experimental investigation.[33] The interactions were filtered for redundancy, potential false positives and isolated components to infer a representative undirected and singly connected high-confidence human protein interactome (HPI) comprising 22 532 nonredundant binary physical interactions between 7277 proteins (see Supporting Information, Figure S2, Table S5b). The inferred HPI was used to identify biologically relevant trends, the significance of which was assessed by using randomized networks (see below). Secondary interactors of the NS5A interacting proteins were retrieved from the HPI and were appended to the NS5A–host interactions to construct a representative NS5A infection network (Supporting Information, Table S5a).

Topological Analysis

Network components were visualized using Cytoscape,[34,35] while network properties such as *node degree distribution*, *average shortest path* and *betweenness* measures were computed using Cytoscape NetworkAnalyzer plugin[36] as described earlier.[24] For comparison, degree preserved randomized PPI networks were generated by edge rewiring using the Cytoscape RandomNetworks plugin and were used as control networks to assess the statistical significance of the topological trends observed in the inferred PPI networks (see Supporting Information).

Functional Analysis by Characterization of Enriched Biological Associations

Protein structural domain assignments were retrieved from the Gene3D database,[37] Gene ontology associations from the GO consortium,[38] and biological pathway data from KEGG[39] were used to assign functional annotations to the genes in the NS5A infection network. The enrichment of specific biological associations within the NS5A infection network was estimated by performing the hypergeometric test within TargetMine. The inferred p-values were further adjusted for multiple test correction to control the false discovery rate using the Benjamini and Hochberg procedure,[40,41] and the annotations/pathways were considered significant if the adjusted $p \leq 0.005$.

RNAi and Transfection

A mixture of four siRNA targets each to RTN1 and RTN3 (SMARTpool:siGENOME RTN1 siRNA and SMARTpool:siGENOME RTN3 siRNA, respectively) were purchased from Thermo Scientific (Thermo Scientific, Waltham, MA, USA). siGENOME Non-Targeting siRNA Pool #1 (Thermo Scientific) was used as a control siRNA. Thermo Scientific ID numbers of siRNA mixtures of RTN1 and RTN3 and the control were M-014138-00, M-020088-00 and D-001206-13-05, respectively. Each siRNA mixture was introduced into the cell lines by using lipofectamine RNAiMax (Invitrogen, Carlsbad, CA, USA). The replicon cell line, as will be described below, was transfected with each siRNA at a final concentration of 20 nM as per the manufacturer's protocol and then seeded at 2.5×10^4 cells per well of a 24-well plate. The transfected cells were harvested at 72 h post-transfection. The Huh7OK1 cell line, as will be described below, was transfected with each siRNA at a final concentration of 20 nM as per the manufacturer's protocol and then seeded at 2.5×10^4 cells per well of a 24-well plate. The transfected cells were infected with JFH1 at an MOI of 0.05 at 24 h post-transfection. The resulting cells were harvested at the indicated time.

Table 1. List of 132 Human Proteins Interacting with the HCV NS5A Protein

gene ID	symbol	description	refs
47	ACLY	ATP citrate lyase	22
60	ACTB	actin, beta	101
79026	AHNAK	AHNAK nucleoprotein	22
10598	AHSA1	AHA1, activator of heat shock 90 kDa protein ATPase homologue 1 (yeast)	102
207	AKT1	v-akt murine thymoma viral oncogene homologue 1	22
302	ANXA2	annexin A2	103
335	APOA1	apolipoprotein A-I	22
348	APOE	apolipoprotein E	22
116985	ARAP1	ArfGAP with RhoGAP domain, ankyrin repeat and PH domain 1	22
27236	ARFIP1	ADP-ribosylation factor interacting protein 1	22
23204	ARL6IP1	ADP-ribosylation factor-like 6 interacting protein 1	this study
4508	ATP6	ATP synthase F0 subunit 6	this study
8312	AXIN1	axin 1	22
581	BAX	BCL2-associated X protein	22
222389	BEND7	BEN domain containing 7	22
274	BIN1	bridging integrator 1	this study; 22,47
89927	C16orf45	chromosome 16 open reading frame 45	this study
8618	CADPS	Ca^{++}-dependent secretion activator	22
93664	CADPS2	Ca^{++}-dependent secretion activator 2	22
79080	CCDC86	coiled-coil domain containing 86	22
983	CDK1	cyclin-dependent kinase 1	22
1021	CDK6	cyclin-dependent kinase 6	22
1060	CENPC1	centromere protein C 1	22
153241	CEP120	centrosomal protein 120 kDa	22
11190	CEP250	centrosomal protein 250 kDa	22
9702	CEP57	centrosomal protein 57 kDa	22
80254	CEP63	centrosomal protein 63 kDa	22
1381	CRABP1	cellular retinoic acid binding protein 1	22
1445	CSK	c-src tyrosine kinase	22
1452	CSNK1A1	casein kinase 1, alpha 1	104
1457	CSNK2A1	casein kinase 2, alpha 1 polypeptide	63,105
1499	CTNNB1	catenin (cadherin-associated protein), beta 1, 88 kDa	84,106
9093	DNAJA3	DnaJ (Hsp40) homologue, subfamily A, member 3	22
2202	EFEMP1	EGF containing fibulin-like extracellular matrix protein 1	22
5610	EIF2AK2	eukaryotic translation initiation factor 2-alpha kinase 2	22
2051	EPHB6	EPH receptor B6	this study
54942	FAM206A	family with sequence similarity 206, member A	22
25827	FBXL2	F-box and leucine-rich repeat protein 2	22
2274	FHL2	four and a half LIM domains 2	22
23770	FKBP8	FK506 binding protein 8, 38 kDa	this study; 43,45
2316	FLNA	filamin A, alpha	12
2495	FTH1	ferritin, heavy polypeptide 1	22
8880	FUBP1	far upstream element (FUSE) binding protein 1	107
2534	FYN	FYN oncogene related to SRC, FGR, YES	22
11345	GABARAPL2	GABA(A) receptor-associated protein-like 2	this study
54826	GIN1	gypsy retrotransposon integrase 1	22
2801	GOLGA2	golgin A2	22
2874	GPS2	G protein pathway suppressor 2	22
2885	GRB2	growth factor receptor-bound protein 2	22
2931	GSK3A	glycogen synthase kinase 3 alpha	22
2932	GSK3B	glycogen synthase kinase 3 beta	22
3055	HCK	hemopoietic cell kinase	22
3320	HSP90AA1	heat shock protein 90 kDa alpha (cytosolic), class A member 1	22
3303	HSPA1A	heat shock 70 kDa protein 1A	108
3315	HSPB1	heat shock 27 kDa protein 1	109
3537	IGLC1	immunoglobulin lambda constant 1 (Mcg marker)	22
79711	IPO4	importin 4	22
3843	IPO5	importin 5	22
3683	ITGAL	integrin, alpha L (antigen CD11A (p180), lymphocyte function-associated antigen 1; alpha polypeptide)	22
6453	ITSN1	intersectin 1	this study
3716	JAK1	Janus kinase 1	22

Table 1. continued

gene ID	symbol	description	refs
3932	LCK	lymphocyte-specific protein tyrosine kinase	22
55679	LIMS2	LIM and senescent cell antigen-like domains 2	22
4067	LYN	v-yes-1 Yamaguchi sarcoma viral related oncogene homologue	22
9448	MAP4K4	mitogen-activated protein kinase kinase kinase kinase 4	this study
6300	MAPK12	mitogen-activated protein kinase 12	22
4155	MBP	myelin basic protein	22
4256	MGP	matrix Gla protein	110
55233	MOB1A	MOB kinase activator 1A	22
4673	NAP1L1	nucleosome assembly protein 1-like 1	22
4674	NAP1L2	nucleosome assembly protein 1-like 2	22
10397	NDRG1	N-myc downstream regulated 1	22
4778	NFE2	nuclear factor (erythroid-derived 2), 45 kDa	22
11188	NISCH	nischarin	this study
4924	NUCB1	nucleobindin 1	22
4938	OAS1	2′-5′-oligoadenylate synthetase 1, 40/46 kDa	22
5007	OSBP	oxysterol binding protein	111
64098	PARVG	parvin, gamma	22
5170	PDPK1	3-phosphoinositide dependent protein kinase-1	22
5297	PI4KA	phosphatidylinositol 4-kinase, catalytic, alpha	22
5291	PIK3CB	phosphoinositide-3-kinase, catalytic, beta polypeptide	22
5295	PIK3R1	phosphoinositide-3-kinase, regulatory subunit 1 (alpha)	55,84,106
5300	PIN1	peptidylprolyl cis/trans isomerase, NIMA-interacting 1	112
5307	PITX1	paired-like homeodomain 1	22
5347	PLK1	polo-like kinase 1	113
10654	PMVK	phosphomevalonate kinase	22
5478	PPIA	peptidylprolyl isomerase A (cyclophilin A)	114,115
10848	PPP1R13L	protein phosphatase 1, regulatory subunit 13 like	22
5515	PPP2CA	protein phosphatase 2, catalytic subunit, alpha isozyme	116
5518	PPP2R1A	protein phosphatase 2, regulatory subunit A, alpha	116
5698	PSMB9	proteasome (prosome, macropain) subunit, beta type, 9 (large multifunctional peptidase 2)	22
5757	PTMA	prothymosin, alpha	22
5894	RAF1	v-raf-1 murine leukemia viral oncogene homologue 1	22
6142	RPL18A	ribosomal protein L18a	22
6167	RPL37	ribosomal protein L37	this study
6238	RRBP1	ribosome binding protein 1 homologue 180 kDa (dog)	22
91543	RSAD2	radical S-adenosyl methionine domain containing 2	117
6252	RTN1	reticulon 1	this study
10313	RTN3	reticulon 3	this study
6424	SFRP4	secreted frizzled-related protein 4	22
81858	SHARPIN	SHANK-associated RH domain interactor	22
64754	SMYD3	SET and MYND domain containing 3	22
8470	SORBS2	sorbin and SH3 domain containing 2	22
10174	SORBS3	sorbin and SH3 domain containing 3	22
6714	SRC	v-src sarcoma (Schmidt-Ruppin A-2) viral oncogene homologue (avian)	22
10847	SRCAP	Snf2-related CREBBP activator protein	22
6741	SSB	Sjogren syndrome antigen B (autoantigen La)	22
284297	SSC5D	scavenger receptor cysteine rich domain containing (5 domains)	110
6772	STAT1	signal transducer and activator of transcription 1	118
25777	SUN2	Sad1 and UNC84 domain containing 2	this study
6850	SYK	spleen tyrosine kinase	119
4070	TACSTD2	tumor-associated calcium signal transducer 2	22
6880	TAF9	TAF9 RNA polymerase II, TATA box binding protein (TBP)-associated factor, 32 kDa	22
6908	TBP	TATA box binding protein	22
7046	TGFBR1	transforming growth factor, beta receptor 1	22
7057	THBS1	thrombospondin 1	22
374395	TMEM179B	transmembrane protein 179B	22
7110	TMF1	TATA element modulatory factor 1	22
7157	TP53	tumor protein p53	22
7159	TP53BP2	tumor protein p53 binding protein, 2	22
7186	TRAF2	TNF receptor-associated factor 2	22
11078	TRIOBP	TRIO and F-actin binding protein	22

Table 1. continued

gene ID	symbol	description	refs
51061	TXNDC11	thioredoxin domain containing 11	22
53347	UBASH3A	ubiquitin associated and SH3 domain containing A	22
10869	USP19	ubiquitin specific peptidase 19	22
9218	VAPA	VAMP (vesicle-associated membrane protein)-associated protein A, 33 kDa	22
9217	VAPB	VAMP (vesicle-associated membrane protein)-associated protein B and C	this study; 22,28,46
10493	VAT1	vesicle amine transport protein 1 homologue (*T. californica*)	this study
55737	VPS35	vacuolar protein sorting 35 homologue (*S. cerevisiae*)	22
6293	VPS52	vacuolar protein sorting 52 homologue (*S. cerevisiae*)	22
140612	ZFP28	zinc finger protein 28 homologue (mouse)	this study
9726	ZNF646	zinc finger protein 646	22

Quantitative Reverse-Transcription PCR (qRT-PCR)

Total RNA was prepared from the cell and culture supernatant using the RNeasy mini kit (QIAGEN, Hilden, Germany) and QIAamp Viral RNA Mini Kit (QIAGEN), respectively. First-strand cDNA was synthesized using high capacity cDNA reverse transcription kit (Applied biosystems, Carlsbad, CA, USA) with random primers. Each cDNA was estimated by Platinum SYBR Green qPCR Super Mix UDG (Invitrogen) as per the manufacturer's protocol. Fluorescent signals of SYBR Green were analyzed with ABI PRISM 7000 (Applied Biosystems). The HCV internal ribosomal entry site (IRES) region and human glyceraldehyde-3-phosphate dehydrogenase (GAPDH) gene were amplified with the primer pairs 5′-GAGTGTCGTGCAGCCTCCA-3′ and 5′-CACTCG-CAAGCACCCTATCA-3′, and 5′-GAAGGTCGGAGT-CAACGGATT-3′ and 5′-GATGACAAGCTTCCCGTTCTC-3′, respectively.[42] The quantities of the HCV genome and the other host mRNAs were normalized with that of GAPDH mRNA. RTN1 and RTN3 genes were amplified using the primer pairs purchased from QIAGEN.

Cell Lines and Virus Infection

Cells from the Huh7OK1 cell line are highly permissive to HCV JFH1 strain (genotype 2a) infection compared to Huh 7.5.1 and exhibit the highest propagation efficiency for JFH1.[43] These cells were maintained at 37 °C in a humidified atmosphere and 5% CO_2, in the Dulbecco's modified Eagle's medium (DMEM) (Sigma, St. Louis, MO, USA) supplemented with nonessential amino acids (NEAA) and 10% fetal calf serum (FCS). The viral RNA of JFH1 was introduced into Huh7OK1 as described by Wakita et al.[44] The viral RNA of JFH1 derived from the plasmid pJFH1 was prepared as described by Wakita et al.[44]

Statistical Analysis

Experiments for RNAi transfection and qRT-PCR were performed two times. The estimated values were represented as the mean ± standard deviation (n = 2). The significance of differences in the means was determined by the Student's t-test.

RESULTS AND DISCUSSION

Identifying Host Proteins That Interact with HCV NS5A Protein

We employed an integrated approach that combined an experimental Y2H assay and comprehensive literature mining to identify human host proteins interacting with NS5A.

First, we performed an Y2H screening to characterize the interactions between NS5A and host proteins. The analysis of positive colonies revealed 17 host factors as interacting partners of NS5A (Tables 1, S1, Supporting Information), 14 of which are novel. The other three interactions have been characterized previously; vesicle-associated membrane protein (VAMP)-associated protein B (VAPB), a membrane trafficking factor, and FK506-binding protein 8 (FKBP8), an immunoregulation protein, independently regulate HCV replication via interactions with NS5A;[28,43,45,46] Bridging integrator 1 (BIN1), a tumor suppressor protein, interacts with NS5A and significantly contributes to HCC.[47] Among the newly discovered interactors, MAP4K4 is overexpressed in HCC, and knockdown of MAP4K4 expression inhibits HCC progression;[48] RTN1 and VAT1 were previously observed to be elevated in HCV infected cells,[49] and ARL6IP1, EPHB6, GABARAPL2, ITSN1 and NISCH were differentially expressed in HCV infection in vitro.[50] Furthermore, five (ARL6IP1, FKBP8, RTN1, RTN3, VAPB) of the 17 interactors (29.4%) localize to the endoplasmic reticulum (ER; GO:0005783; p = 0.0028), which is consistent with the role of NS5A as a crucial constituent of the HCV replication complex associated with the ER.[51] These results suggest that the PPIs detected by our Y2H assay may closely reflect NS5A interactions in vivo.

We next scanned the biomedical literature to expand the repertoire of NS5A–host interactions. Because of an ever increasing volume of biomedical literature describing the pathogenesis of infectious diseases, the identification of specific host–pathogen interactions and their roles in pathogenicity is a nontrivial task, and therefore, recent years have witnessed a rapid development of computational tools for biomedical literature mining. We performed extensive literature mining using computational tools that facilitate the retrieval and extraction of relevant information from the biomedical literature (Pubmed, EBIMed, Protein Coral) and followed it up with a careful manual inspection to identify additional host factors, which directly interact with NS5A and which were not present in the Y2H data set. One hundred and fifteen pairwise interactions between NS5A and human proteins (consisting of 93 catalogued by a high throughput study of binary HCV–host interactions[22] and 22 from assorted reports; see Supporting Information, Table S2) were extracted from the literature in this manner and were added to the existing interactors. The resulting NS5A–human interactome thus comprised 132 human host proteins directly interacting with NS5A (Table 1), all of which are expressed in the liver (see Supporting Information, Table S3).

Network Topological Analysis of the NS5A–host Interactions: NS5A Preferentially Targets Hubs and Bottlenecks in the Host Protein Interactome

To further understand the biological significance of the NS5A–host interactions, we retrieved PPIs for the nodes targeted by

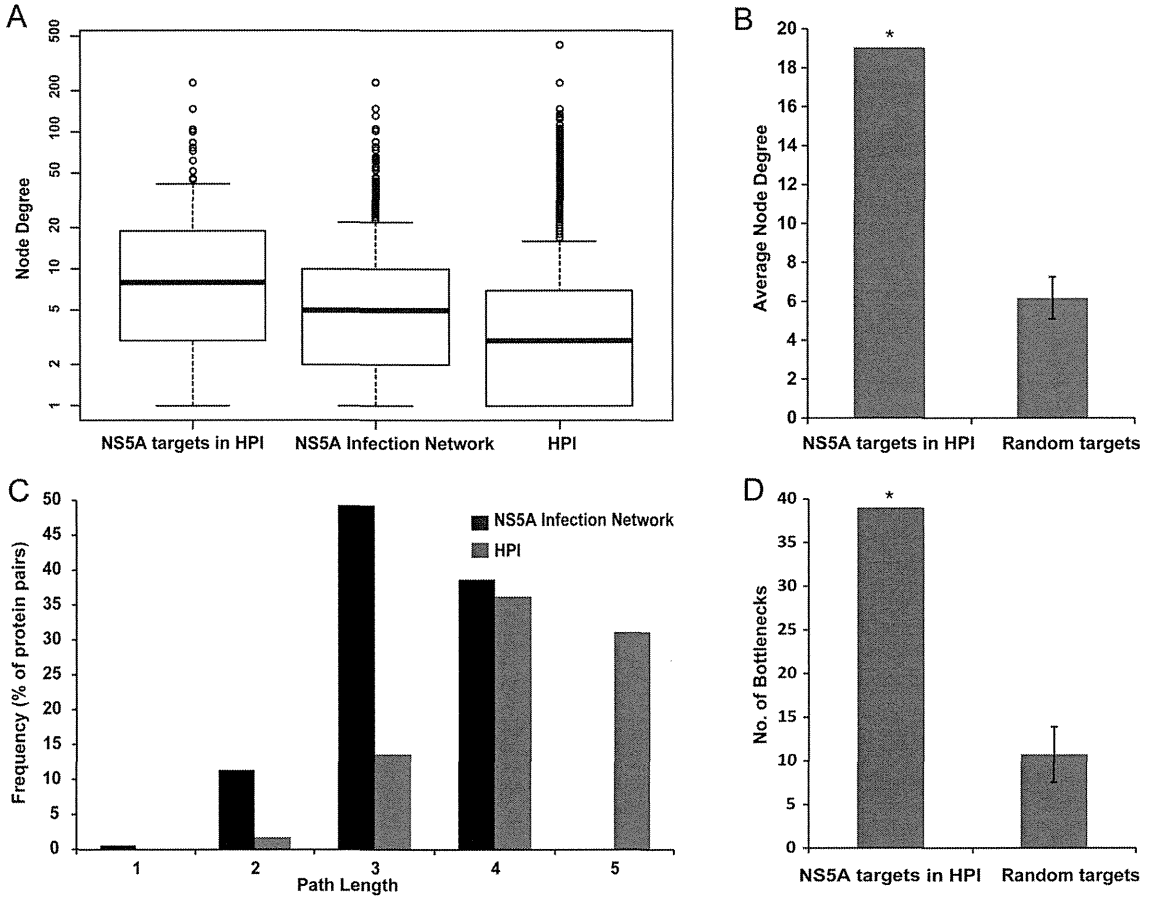

Figure 1. Topological analysis of the NS5A infection network. (A) The node degree distributions of the NS5A interatcors in the HPI, NS5A infection network, and HPI are represented as box plots. The average degree of the NS5A interactors in HPI (19.02) was higher than those of the NS5A infection network (8.24) and HPI (5.96). Median node degrees (indicated by thick horizontal lines) of the NS5A interactors in HPI, NS5A infection network, and HPI are 8, 5, and 3, respectively. (B) The average degree of the nodes targeted by NS5A in HPI was much higher than mean average degree of 1000 sets of the randomly selected 108 nodes in HPI. (C) The shortest path length distributions of the NS5A infection network and HPI. The path length is represented on the x-axis while the y-axis describes the frequency, i.e., the percentage of node (protein) pairs within the PPI network with a given shortest path length. For simplicity, only the node frequencies for path lengths 1−5 in the HPI are displayed. (D) The number of bottlenecks among the nodes targeted by NS5A in HPI was much higher than mean of the number of bottlenecks among 1000 sets of the randomly selected 108 nodes in HPI. *: $p < 0.001$.

NS5A in the HPI and incorporated them with the initial interactions to infer an extended NS5A infection network. PPIs for 108 of 132 NS5A interactors were retrieved in this manner; 24 of 132 NS5A interactors had no PPIs in the HPI (Supporting Information, Tables S4, S5a, S5b). For the NS5A infection network and the HPI, we computed the node degree distribution and the characteristic/average path length measures to capture the topologies of the two networks. The degree of a protein, which corresponds to the number of its interacting partners, may often reflect its biological relevance since a better connected protein is likely to have a higher ability to influence biological networks via PPIs. Average path lengths provide an approximate measure of the relative ease and speed of dissemination of information between the proteins in a network.

The NS5A infection network consisted of 1442 entities (nearly all of which are expressed in the liver; see Supporting Information) with 6263 interactions between them (Supporting Information, Tables S4, S5a). The average degree (defined as the number of interactions for a given protein) of the NS5A infection network (8.24) was notably higher than the degree inferred for the HPI (5.96) (Figure 1A). Furthermore, the average degree of the nodes targeted by NS5A in the HPI (19.02) was even higher; this number is significantly greater than the average degree obtained from a sample of randomly selected nodes (6.17 ± 1.08 with $p < 0.001$; Figure 1B; see Supporting Information). Also the degrees inferred for the majority of the NS5A interactors in the HPI (65 of 108; 60.18%) were higher than the mean degree of the HPI (5.96) (Figure 1A). Our observations therefore suggest that NS5A preferentially targets several highly connected cellular proteins (hubs) with an ability to influence a large number of host factors in HCV infection. The average (shortest) path length of the NS5A infection network (3.26) was significantly shorter than the HPI (4.54), and also the distribution of shortest path lengths was shifted toward the left (Figure 1C), thereby suggesting that the NS5A influenced cellular network is more compact and inclined toward faster communication between the constituents relative to the host cellular network.

Next, we examined the betweenness measures of the NS5A interactors in the HPI to assess their significance in the HPI and the NS5A infection network. The betweenness of a node, determined by the number of shortest paths passing through it, reflects the importance of that node in the network; the nodes

with the highest betweenness prominently regulate the flow of signaling information and are therefore "bottlenecks", representing central points for communication in an interaction network.[52] Previously, proteins with high betweenness have been implicated in crucial roles in HCV infection and pathogenesis.[53,54] To investigate if NS5A preferentially targets bottlenecks (defined as the top 10% of the nodes in the HPI ranked by betweenness), we estimated the fraction of NS5A interactors that were bottlenecks in the HPI. A significant proportion (39 of 108; 36.1%) of the NS5A interactors were identified as bottlenecks in the HPI (Supporting Information, Table S6); this number is significantly higher than the number of bottlenecks among randomly selected nodes (10.72 ± 3.17 with $p < 0.001$; Figure 1D; see Supporting Information). These include growth factor receptor-binding protein 2 (GRB2), which plays an important role in the subversion of host signaling pathways by NS5A;[55] tumor protein 53 (TP53), a key mediator of the oncogenic effect of NS5A in HCV-induced HCC;[56] and tyrosine kinase SRC, which regulates the formation of NS5A-containing HCV replication complex.[57] Among the NS5A interacting proteins identified by our Y2H screening, ITSN1, an endocytic traffic associated protein, and GABARAPL2, an autophagy associated protein, were identified as network bottlenecks.

Our observations therefore suggest that NS5A preferentially interacts with highly central proteins in the host protein interactome; these interactions may help the virus to regulate efficiently the flow of the infection-related information in the host cellular network and manipulate the host metabolic machinery for its own survival and pathogenesis. Our observations are consistent with studies that suggested that viral pathogens tend to interact with well-connected host proteins that are central to the host cellular networks, thus enabling them to appropriate essential cellular functions.[21,22,26,58,59]

Functional Analysis of NS5A Interaction Network

Next, we investigated the NS5A infection network for the enrichment of specific biological associations (KEGG pathways, CATH structural domains; GO terms and Reactome Pathways; Supporting Information, Tables S7a, S7b, S7c and S7d). Notably, a significant proportion of the proteins in the NS5A infection network were mapped to the CATH Phosphorylase Kinase; domain 1, domain (CATH:3.30.200.20; 138 out of 1442, $p = 2.61 \times 10^{-45}$) including 23 of the 132 NS5A interacting host proteins ($p = 3.38 \times 10^{-14}$) (13 of which are bottlenecks in the HPI), based on the Gene3D protein domain assignments (Supporting Information, Table S7b). These include two novel interactions between EPHB6 (a kinase deficient receptor) and MAP4K4 and NS5A, identified by our Y2H assay (Table 1). The significant representation of cellular kinases in the NS5A infection network is consistent with the key roles played by reversible phosphorylation of NS5A in modulating various NS5A functions in HCV pathogenesis. Impairing NS5A hyperphosphorylation has been shown to inhibit HCV replication, and thus, the cellular kinases that regulate NS5A phosphorylation are important targets for anti-HCV therapy.[9,60−63]

The analysis of NS5A infection network revealed an enrichment of 79 KEGG pathways (Supporting Information, Table S7a). Furthermore, 31 of the 39 NS5A interacting bottlenecks (hereafter referred to as bottlenecks) were mapped to 75 of the 79 enriched KEGG pathways (Supporting Information, Table S5). Among the 75 bottleneck-associated enriched KEGG pathways, the highest numbers were associated with various cancers and infectious diseases (31 enriched KEGG pathways; 27 bottlenecks), followed by immune system, signal transduction and endocrine system (23 enriched KEGG pathways; 27 bottlenecks), cell growth and death (4 enriched KEGG pathways; 9 bottlenecks), nervous system (4 enriched KEGG pathways; 8 bottlenecks) and cellular communication (3 enriched KEGG pathways; 14 bottlenecks) among others (Tables 2, S8a, Supporting Information). Below we describe our observations on the most prominent enriched biological themes of interest that were associated with the NS5A infection network, with a specific focus on the bottlenecks.

Cancers and Infectious Diseases

The analysis of the NS5A interaction network revealed that NS5A specifically targets host factors that participate in various complex human diseases. Thirty-four NS5A interactors including 24 bottlenecks were mapped to one or more of the 17 enriched KEGG pathways associated with different infectious diseases (Supporting Information, Tables S7a, S8a). Among the most prominent associations, 12 bottlenecks were mapped to "Epstein−Barr virus infection" ($p = 1.36 \times 10^{-27}$); 10 to "Hepatitis C" ($p = 3.47 \times 10^{-24}$); 10 to "HTLV-I infection" ($p = 1.39 \times 10^{-20}$); 9 to "Hepatitis B" ($p = 3.33 \times 10^{-26}$); 8 to "Measles" ($p = 5.69 \times 10^{-17}$); 7 bottlenecks were mapped to "Influenza A" ($p = 5.01 \times 10^{-12}$); 7 to "Herpes simplex infection" ($p = 1.47 \times 10^{-13}$) and 6 to "Tuberculosis" ($p = 3.02 \times 10^{-6}$) (Supporting Information, Tables S7a, S8a). These associations include infectious diseases induced by various bacterial and viral pathogens thereby suggesting that HCV and other pathogens may systematically target specific host factors, the perturbation of which may contribute to the onset of various human diseases.

Also, 19 bottlenecks were mapped to one or more of the 16 enriched KEGG pathways associated with various cancers. Among the most prominent associations, 10 bottlenecks were mapped to "Viral carcinogenesis" ($p = 1.3 \times 10^{-30}$); 8 each were mapped to "Prostrate cancer" ($p = 4.27 \times 10^{-25}$), "Endometrial cancer" ($p = 5.52 \times 10^{-21}$) and "Colorectal cancer" ($p = 4.22 \times 10^{-18}$); 7 to "Pancreatic cancer" ($p = 1.94 \times 10^{-18}$); 6 to "Chronic myeloid leukemia" ($p = 1.61 \times 10^{-30}$) and 5 each to "Non-small cell lung cancer" ($p = 8.66 \times 10^{-15}$) and "Glioma" ($p = 2.38 \times 10^{-14}$) (Supporting Information, Tables S7a, S8a). The significant association of HCV with host factors central to various cancer pathways (including tumor suppressors such as TP53) is consistent with previous observations that viral pathogens significantly targeted host proteins associated with cancer pathways,[59,64,65] which likely plays major roles in tumorigenesis.

Immune System and Signal Transduction

HCV infection induces various active and passive host immune responses including the recognition of viral RNA by host cell receptors. These events lead to the production of Type I interferons (IFN-α/β) and inflammatory cytokines in the infected hepatocytes, initiating the antiviral response. HCV persistence in the host is determined by the virus's ability to impair host immune responses.[66−69]

The analysis of the NS5A interaction network revealed that 21 of the 132 NS5A interacting proteins, including 16 bottlenecks and their interacting partners, were mapped to one or more enriched KEGG pathways associated with the immune system (Supporting Information, Tables S7a, S8a).

Table 2. KEGG Pathway Functional Categories (Subclasses) Sorted by the Number of Enriched Pathways (≥3) Associated with One or More NS5A Interacting Bottlenecks

category	no. of enriched pathways	no. of bottle-necks	associated bottlenecks	KEGG pathways in the given category associated with most number of bottlenecks
infectious diseases	16	24	ACTB, AKT1, CDK1, CSNK2A1, CTNNB1, FLNA, FYN, GPS2, GRB2, GSK3B, HSPB1, JAK1, LCK, LYN, PIK3R1, PPP2CA, RAF1, SRC, STAT1, SYK, TBP, TGFBR1, TP53, TRAF2	"Epstein–Barr virus infection"; "HTLV-I infection"; "Hepatitis C"; "Hepatitis B"; "Measles"; "Influenza A"; "Herpes simplex infection"; "Tuberculosis"; "Toxoplasmosis"; "Chagas disease (American trypanosomiasis)"; "Bacterial invasion of epithelial cells"
cancers	16	19	AKT1, AXIN1, CDK1, CTNNB1, GRB2, GSK3B, HSP90AA1, JAK1, LYN, RAF1, SRC, STAT1, SYK, TBP, TGFBR1, THBS1, TP53, TRAF2	"Pathways in cancer"; "Viral carcinogenesis"; "Prostate cancer"; "Endometrial cancer"; "Colorectal cancer"; "Pancreatic cancer"; "Chronic myeloid leukemia"; "Non-small cell lung cancer"; "Glioma"; "Small cell lung cancer"; "Renal cell carcinoma"; "Melanoma"; "Acute myeloid leukemia"
immune system	10	16	ACTB, AKT1, CTNNB1, FYN, GRB2, GSK3B, HSP90AA1, LCK, LYN, PIK3R1, PIN1, RAF1, SRC, STAT1, SYK, TRAF	"Chemokine signaling pathway"; "T cell receptor signaling pathway"; "Fc epsilon RI signaling pathway"; "B cell receptor signaling pathway"; "Natural killer cell mediated cytotoxicity"; "Fc gamma R-mediated phagocytosis"
signal transduction	9	22	AKT1, AXIN1, CSKN1A1, CTNNB1, FLN, GRB2, GSK3B, HSP90AA1, HSPB1, JAK1, LCK, LYN, PIK3R1, PPP2CA, RAF1, SRC, STAT1, SYK, TGFBR1, THBS1, TP53, TRAF2	"PI3K-Akt signaling pathway"; "MAPK signaling pathway"; "Wnt signaling pathway"; "ErbB signaling pathway"; "VEGF signaling pathway"; "NF-kappa B signaling pathway"; "Jak-STAT signaling pathway"
nervous system	5	8	AKT1, GRB2, GSK3B, LYN, PIK3R1, PPP2CA, RAF1, TP53	"Neurotrophin signaling pathway"; "Long-term depression"; "Dopaminergic synapse"; "Long-term potentiation"
endocrine system	4	10	AKT1, CDK1, GRB2, GSK3B, HSP90AA1, PIK3R1, PLK1, RAF1, SRC, TRAF2	"Progesterone-mediated oocyte maturation"; "Insulin signaling pathway"; "GnRH signaling pathway"; "Adipocytokine signaling pathway"
cell growth and death	4	9	AKT1, CDK1, GSK3B, PIK3R1, PLK1, PPP2CA, THBS1, TP53, TRAF2	"Cell cycle"; "Apoptosis"; "p53 signaling pathway"; "Oocyte meiosis"
cell communication	3	14	ACTB, AKT1, CSNK2A1, CTNNB1, FLNA, FYN, GRB2, GSK3B, PIK3R1, PPP2CA, RAF1, SRC, TGFBR1, THBS1	"Focal adhesion"; "Tight junction"; "Adherens junction"
development	3	12	AKT1, FHL2, FYN, GRB2, GSK3B, JAK1, LCK, PIK3R1, STAT1, SYK, TGFBR1, THBS1	"Osteoclast differentiation"; "Axon guidance"; "Dorso-ventral axis formation"

Eight bottlenecks were mapped to the enriched KEGG pathway "Chemokine signaling pathway" ($p = 2.27 \times 10^{-10}$), which is consistent with the modulation of host interferon signaling by NS5A in HCV infection.[70] In addition, 7 bottlenecks each were mapped to "T cell receptor signaling pathway" ($p = 4.6 \times 10^{-24}$), "Fc epsilon RI signaling pathway" ($p = 2.86 \times 10^{-14}$) and "B cell receptor signaling pathway" ($p = 1.8 \times 10^{-14}$) and 6 bottlenecks were mapped to "Natural killer cell mediated cytotoxicity" ($p = 1.92 \times 10^{-12}$). Three bottlenecks (AKT1, PIK3R1 and STAT1) were also mapped to the enriched KEGG pathway "Toll-like receptor signaling pathway" ($p = 3.23 \times 10^{-7}$; Supporting Information, Tables S7a, S8a). Toll-like receptor 3 mediated chemokine and cytokine signaling plays an important role in the host immune response in HCV infection.[71] Therefore, NS5A interaction with bottlenecks, which function in various aspects of the host immune response, may significantly contribute to the perturbation of the host immune system in HCV pathogenesis.

Additionally, 32 of 132 NS5A interacting proteins examined in the present study, including 24 bottlenecks, were mapped to various pathways associated with the signal transduction and the endocrine system (Supporting Information, Tables S7a, S8a), many of which are implicated in HCV infection and HCC progression and are targets for molecular therapy in HCC.[22,72−74]

Eleven bottlenecks were mapped to the enriched KEGG pathway "PI3K-Akt signaling pathway" ($p = 2.2 \times 10^{-24}$; Supporting Information, Tables S7a, S8a), which is consistent with a previous study that NS5A stimulates the activation of PI3K-Akt pathway, which contributes to HCC in HCV infection.[75] Eight bottlenecks were mapped to the enriched KEGG pathway "MAPK signaling pathway" ($p = 2.4 \times 10^{-19}$; Supporting Information, Tables S7a, S8a). Elements of the MAPK signaling cascades are directly involved in the progression of HCV infection, particularly in association with HCV Core and E2 proteins,[22,24,76,77] thereby suggesting that NS5A interactions with the key facilitators of MAPK signaling in the host interactome may play an important role in regulating the reversible phosphorylation of NS5A and may contribute to the progression of HCV pathogenesis.

Bottlenecks AKT1, GRB2, GSK3B, PIK3R1 and RAF1 and many of their interactors were mapped to the enriched KEGG pathway "Insulin signaling pathway" ($p = 2.42 \times 10^{-13}$; Supporting Information, Tables S7a, S8a); these proteins are highlighted in Figure 2. Insulin signaling plays an important role in regulating glucose and lipid metabolism, and the disruption of this process may contribute to insulin resistance (IR). IR is linked with steatosis, fibrosis progression and poor interferon-α response in HCV infection.[78−80] Suppression of AKT1 and GSK3B activity in HCV infection disrupts glucose metabolism and contributes to IR.[81,82] Furthermore, PIK3R1 and NS5A interactor PIK3CB (Figure 2) are subunits of phosphatidylinositol 3-kinase (PI3K), which controls insulin secretion;[83] PI3K also facilitates the activation of the proto-oncogene beta-catenin (CTNNB1) by NS5A, which contributes to the development of HCC in HCV pathogenesis.[84] Previously, HCV Core protein has been directly implicated in the induction of IR in HCV infection,[85] while there is little evidence suggesting definitive links between NS5A and IR. Our observations, however, suggest that NS5A directly interacts with key regulators of insulin metabolism and may, therefore, play a major role in modulating HCV-induced IR and eventually HCC.

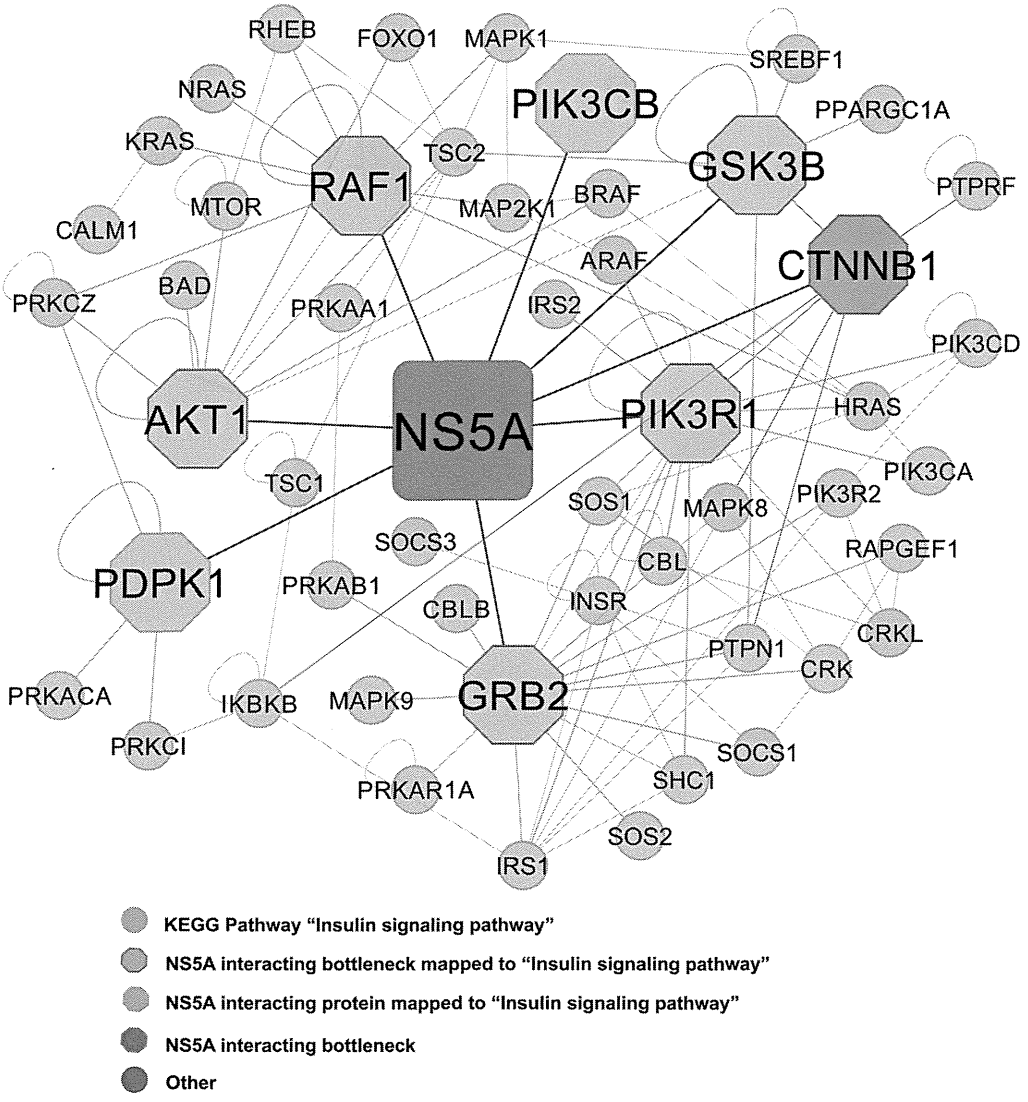

Figure 2. NS5A interacting bottlenecks and their interacting partners associated with the enriched KEGG pathway hsa04910: "Insulin signaling pathway".

Cell Adhesion and Communication

The perturbation of adherens and tight junction associated proteins has been implicated in HCV entry, cell–cell transmission and hepatoma migration in HCV infection.[86−88] In the NS5A infection network, eight bottlenecks (ACTB, AKT1, CSNK2A1, CTNNB1, FYN, PPP2CA, SRC and TGFBR1) were mapped to either or both of the enriched KEGG pathways "Adherens Junction" ($p = 1.03 \times 10^{-15}$) and "Tight junction" ($p = 1.19 \times 10^{-5}$), which are associated with cell adhesion junctions and cellular communication (Supporting Information, Tables S7a, S8a). CSNK2A1 is the catalytic (alpha) subunit of Casein Kinase II (CK2), which phosphorylates NS5A and regulates the production of infectious viral particles.[63] CTNNB1, a key component of cell-adhesion complexes, is positively regulated by CK2.[89] Furthermore, the activation of CTNNB1 by NS5A significantly contributes to HCC.[84] Taken together, our observations suggest that NS5A interactions with bottlenecks, which regulate cell–cell adhesion (CSNK2A1, CTNNB1) and cytoskeletal organization (ACTB), may significantly contribute to the progression of HCV life cycle and tumorigenesis in HCV pathogenesis.

Eleven bottlenecks were mapped to the enriched KEGG pathway "Focal Adhesion" ($p = 1.02 \times 10^{-17}$; Supporting Information, Tables S7a, S8a), thereby reiterating that focal adhesion is a major target of NS5A.[22] Focal adhesion regulates cell migration and adhesion, and some of its components were directly implicated in the regulation of HCV replication and propagation in our earlier study.[24] Our observations thus suggest that NS5A interactions with key components of the focal adhesion machinery may play important roles in the HCV lifecycle. For instance, NS5A interacts with bottleneck THBS1 (Thrombospondin-1), a glycoprotein, which was mapped to the KEGG "Focal Adhesion" pathway. THBS1 plays a key role in NS5A-mediated activation of the cytokine TGF-β1, which facilitates HCV replication and progressive liver fibrosis in HCV infection.[90] Our observations suggest that direct NS5A interactions with the bottlenecks THBS1 and TGFBR1 (TGF-β receptor 1; KEGG Pathway "Adherens Junction"), a key facilitator of TGF-β downstream signaling, may be crucial in facilitating HCV replication and tumorigenesis in HCV pathogenesis.

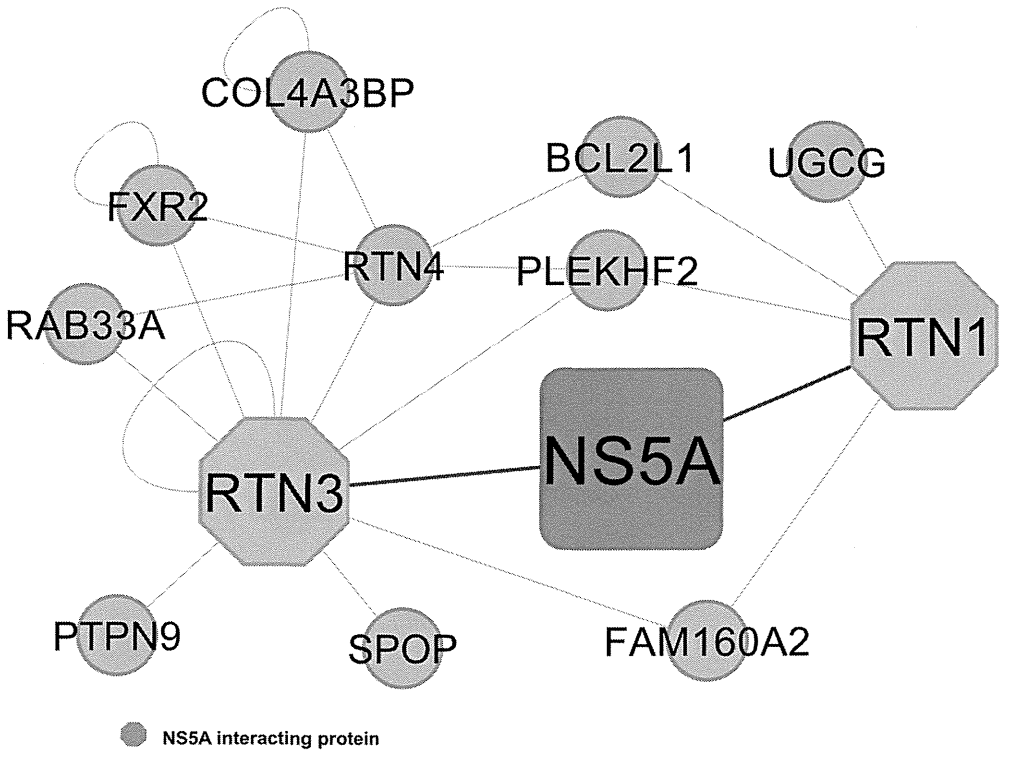

Figure 3. ER-localized host factors RTN1 and RTN3 were found to interact (blue edges) with NS5A in an Y2H screening of human liver cDNA library using NS5A as bait.

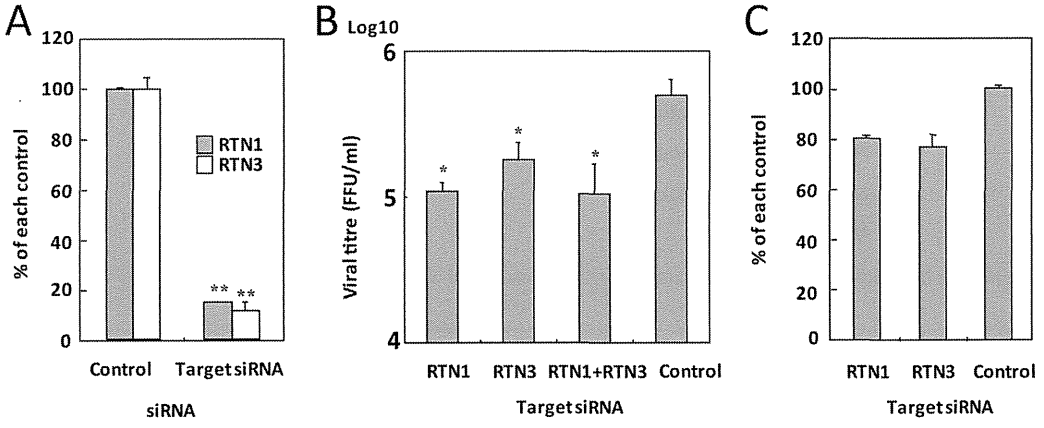

Figure 4. Effects of knockdown of RTN1 and RTN3 on HCV propagation and replication. Host factors RTN1 and RTN3 were suppressed by RNAi (A) in Huh7OK1 cells infected with HCV JFH1 strain (genotype 2a). The amounts of viral titer (B) and intracellular viral RNA (C) were estimated. Each value was represented as percentage of the cells transfected with the control siRNA. FFU: Focus-forming units; *: $p < 0.05$, **: $p < 0.01$.

Cellular Transport

Cellular factors associated with endocytic trafficking are key facilitators of the HCV life cycle, particularly HCV entry into the hepatic cells.[91−93] Endocytosis of the extracellular growth factor receptor (EGFR) in association with the cell surface glycoprotein CD81 plays a crucial role in HCV internalization and entry and is, therefore, an attractive target of anti-HCV strategies.[94] In the NS5A infection network, NS5A interactors ARAP1 and HSPA1A together with two bottlenecks (SRC, TGFBR1) were mapped to the enriched KEGG pathway "Endocytosis" ($p = 2.97 \times 10^{-8}$; Supporting Information, Tables S7a, S8a). ARAP1, a Golgi associated protein, negatively regulates EGFR trafficking, and decreased ARAP1 expression contributes to enhanced EGFR endocytosis.[95] Therefore, NS5A interaction with ARAP1 may facilitate EGFR internalization and thus viral entry in HCV infection.

NS5A Interacting Host Proteins RTN1 and RTN3 Function in HCV Propagation but Not Replication

Traditionally, viral and host proteins associated with the HCV lifecycle (internalization, replication, assembly and release) have been preferred targets in the anti-HCV studies. During infection, HCV localizes to the detergent-resistant membrane fraction (DRM) derived from the ER, where the viral replication and assembly take place.[4] Thus, of the novel interactions identified in our Y2H assay, we focused on two ER-localized host factors RTN1 and RTN3 (Figure 3). RTN1 and RTN3 belong to a group of proteins named Reticulons, which are integral to maintaining the shape and organization of the